

# Making Models Unmergeable via Scaling-Sensitive Loss Landscape

Minwoo Jang<sup>1</sup> Hoyoung Kim<sup>1</sup> Jabin Koo<sup>2</sup> Jungseul Ok<sup>1,2</sup>

## Abstract

The rise of model hubs has made it easier to access reusable model components, making model merging a practical tool for combining capabilities. Yet, this modularity also creates a *governance gap*: downstream users can recompose released weights into unauthorized mixtures that bypass safety alignment or licensing terms. Because existing defenses are largely post-hoc and architecture-specific, they provide inconsistent protection across diverse architectures and release formats in practice. To close this gap, we propose TRAP<sup>2</sup>, an architecture-agnostic protection framework that encodes protection into the update during fine-tuning, regardless of whether they are released as adapters or full models. Instead of relying on architecture-dependent approaches, TRAP<sup>2</sup> uses weight re-scaling as a simple proxy for the merging process. It keeps released weights effective in standalone use, but degrades them under re-scaling that often arises in merging, undermining unauthorized merging.

## 1. Introduction

Public model hubs and open repositories, such as GitHub and Hugging Face, widely distribute fine-tuned updates, from full checkpoints to lightweight adapters. Since many updates target the same base model, they can be recombined after release by directly composing their parameters. This accessibility enables model merging, but it also creates a *governance gap*: once released, these updates can be recomposed into unauthorized mixtures that bypass safety, licensing, or task-specific constraints. In other words, facilitating broad reuse inherently reduces the ability to enforce post-release constraints.

This loss of control motivates the notion of *unmergeability* (Junhao et al., 2025; Wang et al., 2025). Ideally, a released model should retain full utility in its standalone setting,

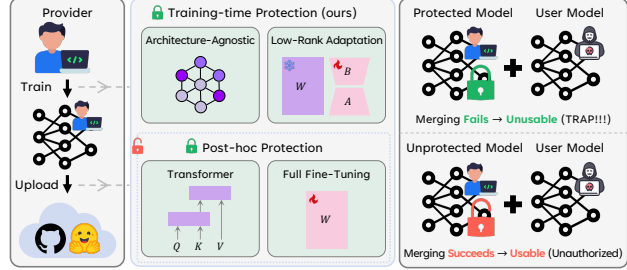


Figure 1. Unmergeability protection in model sharing and limitations of prior work. (Left) Providers release task updates for downstream reuse, often as adapters. (Middle) Most post-hoc protections are Transformer-specific, limiting transfer beyond Transformers. They also require full-weight access, which makes them incompatible with adapter-only releases such as LoRA. (Right) These limitations motivate training-time protection embedded in the released update, preserving standalone utility while making downstream merges unreliable.

while failing reliably when incorporated into unauthorized merges. However, achieving this goal is challenging, because merging is performed downstream, outside the control of the creator, and often under heterogeneous protocols.

Most existing defenses address this challenge in a *post-hoc* manner: they apply function-preserving transformations to disrupt merging without changing the fine-tuning pipeline (Junhao et al., 2025; Wang et al., 2025). However, most existing methods are tailored to architectural symmetries of Transformers (Vaswani et al., 2017), which limits their transferability to non-Transformer backbones. Moreover, they assume access to the *full* model weights, making them mismatched with hub-style releases where only adapter updates, exemplified by Low-Rank Adaptation (LoRA) (Hu et al., 2022), are shared and the base weights are unavailable. Figure 1 summarizes this model-sharing workflow and highlights these two gaps in existing post-hoc defenses.

Against this background, we ask: *Can unmergeability be embedded directly into fine-tuned parameters across architectures and release formats?* We answer yes with TRAP<sup>2</sup> (**T**raining-time **P**rotection via **T**ask-**R**obust **A**dversarial **P**erturbation), which learns a protected update during fine-tuning. Conceptually, TRAP<sup>2</sup> optimizes an adversarial objective over update rescaling: as illustrated in Figure 2, it preserves utility at the authorized scale ( $s = 1$ ), while inducing degradation under unauthorized scaling ( $s \neq 1$ ), a

<sup>1</sup>Graduate School of AI, POSTECH, Pohang, Republic of Korea

<sup>2</sup>Department of CSE, POSTECH, Pohang, Republic of Korea. Correspondence to: Jungseul Ok <jungseul@postech.ac.kr>.

regime that frequently appears in merging pipelines. Consequently, TRAP<sup>2</sup> yields brittleness under merging for both adapter-only and full-checkpoint releases, without relying on architecture-specific assumptions.

In summary, our contributions are as follows:

- **Problem Setup:** We formalize a post-release protection setting for fine-tuned releases across various architectures and release formats (adapter-only updates and full checkpoints), together with a unified evaluation protocol that quantifies standalone utility and degradation under merging.
- **Protection Method:** We introduce TRAP<sup>2</sup>, a training-time procedure that keeps a fine-tuned update effective at the nominal scale ( $s = 1$ ), while making it brittle under *off-nominal re-scaling* ( $s \neq 1$ ), which captures the re-weighting effects commonly introduced by practical merging pipelines.
- **Empirical and Theoretical Analysis:** We evaluate TRAP<sup>2</sup> across diverse merging operators, release formats, and architectures, and complement the empirical results with theoretical analysis, establishing (i) convergence under stochastic optimization and (ii) degradation under down-scaling and model merging.

## 2. Related Works

### 2.1. Model Merging

Model merging aims to compose multiple task-specific models into a single model, with little or no additional training. Early research has focused on full-model merging, where multiple checkpoints are linearly combined. Representative methods include Task Arithmetic (TA) (Ilharco et al., 2023), TIES-Merging (Yadav et al., 2023), and DARE (Yu et al., 2024), which aggregate task updates via weighted summation, often coupled with pruning or sign-conflict resolution.

In parallel, Low-Rank Adaptation (LoRA) (Hu et al., 2022) has emerged as the de facto standard for parameter-efficient fine-tuning. As LoRA adapters are widely shared, merging has naturally extended to the adapter setting. While general merging operators are often directly applied to adapters, recent works, such as KnOTS (Stoica et al., 2025) and Core Space (Panariello et al., 2025), propose merging schemes specifically tailored for low-rank subspaces.

While these developments make downstream reuse increasingly convenient, they also widen a *governance gap*. Post-release merging can obscure provenance and dilute license, IP, or safety constraints by blending protected adapters into composite models (Cong et al., 2024; Xu et al., 2025; Rosati et al., 2024; Hammoud et al., 2024). This vulnerability motivates protection mechanisms that preserve standalone utility

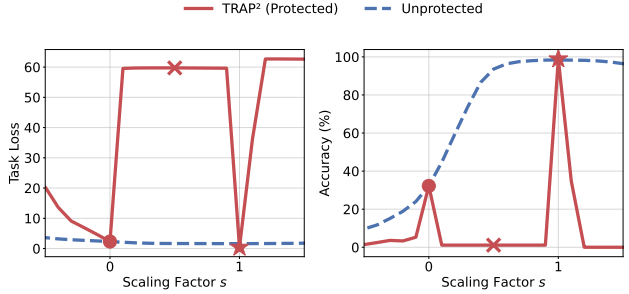


Figure 2. (Left) Loss shaping over the scaling factor  $s$ . We optimize via TRAP<sup>2</sup> to retain high utility in the *authorized* scale (★;  $s = 1$ ), while inducing degradation under *unauthorized* scales (X;  $s \neq 1$ ). The zero-shot result (●;  $s = 0$ ) is shown as a reference. (Right) Accuracy along the scaling factor  $s$ . TRAP<sup>2</sup>-trained adapter attains high standalone accuracy in the authorized region (★) but collapses under unauthorized scaling (X).

while making unauthorized recomposition unreliable.

### 2.2. Unmergeability for Model Protection

Unmergeability aims to keep released weights useful in isolation, while making unauthorized merging unreliable. This capability is vital for model supply-chain control, since recomposition can obscure provenance and complicate the enforcement of usage terms. Existing defenses typically take a *post-hoc* approach, preserving standalone behavior via function-preserving parameter transformations.

PaRaMS (Junhao et al., 2025) and MergeLock (Wang et al., 2025) instantiate this idea for Transformers (Vaswani et al., 2017). They leverage architectural symmetries via coupled transformations of attention projections, preserving standalone behavior, while reducing compatibility under direct weight-space merging. To maintain functional equivalence, they must reparameterize the full set of weights, which makes them incompatible with adapter-only releases (e.g., LoRA) and less transferable to non-Transformer backbones.

In contrast, we target common release settings where full-weight access is unavailable or non-Transformer backbones are used. Accordingly, we propose a training-time mechanism that embeds unmergeability directly into the fine-tuned update, applicable across architectures and release formats, including adapter-only and full-checkpoint releases.

## 3. Background

We briefly review merging protocols to establish the scaling and aggregation notation used in Sections 4 and 5.

**Low-Rank Adaptation (LoRA)** Given a pre-trained model with parameters  $W_0 \in \mathbb{R}^{d_{\text{out}} \times d_{\text{in}}}$ , LoRA (Hu et al., 2022) freezes  $W_0$  and injects trainable low-rank updates into

selected linear layers. Concretely, for  $r \ll \min\{d_{\text{out}}, d_{\text{in}}\}$ ,

$$\Delta W = BA, \quad B \in \mathbb{R}^{d_{\text{out}} \times r}, \quad A \in \mathbb{R}^{r \times d_{\text{in}}}, \quad (1)$$

and the forward-pass weight becomes  $W = W_0 + s \cdot \Delta W$ , where  $s \in \mathbb{R}_{\geq 0}$  denotes a scaling factor applied to the update  $\Delta W$ . The resulting parameters are lightweight and modular, and are commonly released as standalone adapters.

**LoRA Merging** Given  $N$  task-specific LoRA adapters  $\{\Delta W_i\}_{i=1}^N$  trained on the same base model  $W_0$ , LoRA merging aims to compose them into a single adapter without additional training. The most common approach computes a linear aggregation of updates (Ilharco et al., 2023),

$$\Delta W_{\text{merged}} = \sum_{i=1}^N s_i \cdot \Delta W_i, \quad (2)$$

where  $s_i$  denotes the merging coefficient for the  $i^{\text{th}}$  adapter. While recent methods such as KnOTS (Stoica et al., 2025) and Core Space (Panariello et al., 2025) introduce structured subspace projections or alignment steps, they rely on aggregating updates that are (approximately) aligned. We provide a detailed overview of these techniques in Appendix B.

**Unified View: Merging as Aggregating Updates** This perspective also covers full-checkpoint merging. Given checkpoints  $\{W_i\}_{i=1}^N$  derived from the same base  $W_0$ , methods such as TA (Ilharco et al., 2023), TIES-Merging (Yadav et al., 2023), and DARE (Yu et al., 2024) first form task updates  $\Delta W_i := W_i - W_0$  and then merge them (often with pruning or sign-conflict resolution) as

$$W_{\text{merged}} = W_0 + \sum_{i=1}^N s_i \cdot \Delta W_i = W_0 + \Delta W_{\text{merged}}. \quad (3)$$

Throughout this paper, we use  $\Delta W$  to denote a generic released *update* (either a LoRA adapter or a full-parameter difference). We use  $s$  for update scaling, and  $s_i$  for coefficients used to aggregate updates.

## 4. Problem Setup and Challenges

We formalize *unmergeability* under hub-style model sharing and explain why existing post-hoc defenses apply to neither non-Transformer architectures nor adapter releases.

**Loss under Scaling** Let  $\mathcal{D}$  be a data distribution over examples  $\xi$ . We define the expected loss at weights  $W$  as

$$\mathcal{L}(W; \mathcal{D}) := \mathbb{E}_{\xi \sim \mathcal{D}} [\ell(W; \xi)]. \quad (4)$$

When  $\mathcal{D}$  is clear from context, we omit it and write  $\mathcal{L}(W)$ . For an update  $\Delta W$  and a scaling factor  $s \in \mathbb{R}_{\geq 0}$ , define

$$\begin{aligned} \mathcal{L}_{\text{scaled}}(\Delta W; s) &:= \mathcal{L}(W_0 + s \cdot \Delta W) \\ &= \mathbb{E}_{\xi \sim \mathcal{D}} [\ell(W_0 + s \cdot \Delta W; \xi)]. \end{aligned} \quad (5)$$

We take  $s = 1$  as the *nominal* (standalone) scale, and interpret  $s \neq 1$  as off-nominal re-scaling induced by downstream reuse and merging. Accordingly, the intended composition is  $W_0 + \Delta W$ , and  $\mathcal{L}_{\text{nominal}}(\Delta W) := \mathcal{L}_{\text{scaled}}(\Delta W; 1)$ . In Section 5, we will also consider off-nominal scales ( $s \neq 1$ ).

**Merging Operator** Let  $\mathcal{M}(\cdot)$  denote a merging operator that composes a set of updates into a single merged one. Given  $N$  adapters  $\{\Delta W_i\}_{i=1}^N$  trained on the same base  $W_0$ , the merged model is parameterized by

$$W_0 + \Delta W_{\text{merged}}, \quad \Delta W_{\text{merged}} = \mathcal{M}(\{\Delta W_i\}_{i=1}^N). \quad (6)$$

A common instance is linear combination with scaling (Ilharco et al., 2023), as defined in Eq. (2).

**Desired Properties** Our goal is to obtain an update  $\Delta W^*$  that satisfies the following properties established in prior works (Junhao et al., 2025; Wang et al., 2025).

**(Property 1) Standalone Utility:** When deployed alone,  $\Delta W^*$  should incur low loss, i.e.,  $\mathcal{L}_{\text{nominal}}(\Delta W^*)$  is small.

**(Property 2) Unmergeability:** Let  $\mathcal{T} = \{\Delta W_i\}_{i=1}^{N-1}$  be third-party adapters and  $\Delta W_{\text{merged}} := \mathcal{M}(\{\Delta W^*\} \cup \mathcal{T})$ . Define  $\mathcal{L}_{\text{merged}}(\Delta W^*; \mathcal{T}) := \mathcal{L}(W_0 + \Delta W_{\text{merged}})$ . We require that indiscriminate merging yields a substantially worse merged model than merging an *unprotected* update of comparable standalone utility, i.e.,

$$\mathcal{L}_{\text{merged}}(\Delta W^*; \mathcal{T}) \gg \mathcal{L}_{\text{merged}}(\Delta W'; \mathcal{T}), \quad (7)$$

where  $\Delta W'$  is an unprotected adapter for the same task with  $\mathcal{L}_{\text{nominal}}(\Delta W') \approx \mathcal{L}_{\text{nominal}}(\Delta W^*)$ .

**Post-hoc Defenses via Paired Cancellations** Most prior unmergeability defenses are *post-hoc*: they apply function-preserving re-parameterizations to the *full* model weights, preserving standalone behavior while disrupting direct weight-space merging. Two common symmetry templates are: **(i) FFN hidden-unit permutation**, which permutes intermediate neurons and compensates in adjacent linear layers; and **(ii) coupled self-attention reparameterization**, which exploits cancellation structures in Transformers (Vaswani et al., 2017). Concretely, with  $Q = XW_Q$ ,  $K = XW_K$ , and  $V = XW_V$ , the attention output is

$$\text{Attention}(X) = \text{softmax}\left(\frac{QK^\top}{\sqrt{d}}\right) VW_O.$$

A paired invertible re-parameterization preserves the computation by keeping  $QK^\top$  and  $VW_O$  invariant:

$$W_Q \mapsto W_Q R_1, \quad W_K \mapsto W_K R_1^{-\top},$$

$$W_V \mapsto W_V R_2, \quad W_O \mapsto R_2^{-1} W_O,$$

for invertible  $(R_1, R_2)$ .

---

**Algorithm 1** Pseudo-code of TRAP<sup>2</sup> (Adapter Version)
 

---

```

1: Input: fixed base model  $W_0$ , dataset  $\mathcal{D}$ , time step  $T$ ,  

   step sizes  $\{\eta_t\}_{t=0}^{T-1}$ , trade-off weight  $\lambda$ , scale range  

    $[s_{\min}, s_{\max}]$ , exclusion width  $\delta$ , weighting function  $w(\cdot)$ 
2: Initialize a trainable LoRA adapter  $\Delta W$ 
3: for  $t = 0, 1, \dots, T - 1$  do
4:   Sample mini-batch  $\mathcal{B}_t \sim \mathcal{D}$   $(\mathcal{B}_t = \{\xi_j\}_{j=1}^m)$ 
5:    $\mathcal{L}_{\text{nominal}} \leftarrow \frac{1}{m} \sum_{\xi \in \mathcal{B}_t} \ell(W_0 + \Delta W; \xi)$ 
6:   Draw  $s \sim \text{Unif}([s_{\min}, 1 - \delta] \cup [1 + \delta, s_{\max}])$ 
7:    $\mathcal{L}_{\text{off}} \leftarrow \frac{1}{m} \sum_{\xi \in \mathcal{B}_t} w(s) \cdot \ell(W_0 + s \cdot \Delta W; \xi)$ 
8:    $J_t \leftarrow \mathcal{L}_{\text{nominal}} - \lambda \cdot \mathcal{L}_{\text{off}}$ 
9:    $\Delta W \leftarrow \Delta W - \eta_t \cdot \nabla_{\Delta W} J_t$ 
10: end for
11: Output: protected adapter  $\Delta W^*$ 
    
```

---

PaRaMS (Junhao et al., 2025) combines MLP-level rearrangement with attention-level reweighting within this paired-cancellation framework. MergeLock (Wang et al., 2025) adopts a more expressive variant by composing random mixing, permutation, and diagonal reweighting to construct  $R_1$  and  $R_2$ , while still relying on the same paired cancellations. In both cases, the function-preserving guarantee fundamentally assumes access to the full weight tensors on which the paired transformations act.

**Challenges** Modern hub ecosystems present two practical realities: (i) adapter-only release exemplified by LoRA, and (ii) architectural diversity beyond Transformers. These realities expose fundamental flaws in post-hoc defenses. First, applying paired transformations solely to the adapter  $\Delta W$  fails to cancel terms associated with the frozen base model  $W_0$ . This misalignment either degrades standalone utility or fails to induce the intended unmergeability. Second, their symmetry templates are Transformer-specific and do not transfer to non-attention backbones such as ResNet (He et al., 2015) or ConvNeXt (Liu et al., 2022). These limitations motivate our central question: *Can we inject unmergeability directly into the released update, without relying on base-model access or architecture-specific symmetries?*

## 5. Proposed Method

To enforce unmergeability without sacrificing standalone utility, we propose TRAP<sup>2</sup>, a training-time protection objective that directly shapes the released update. We first present the adapter (e.g., LoRA) instantiation in Algorithm 1. The central intuition is to regularize the adapter so that it remains accurate at the nominal scale ( $s = 1$ ) yet degrades under off-nominal scaling ( $s \neq 1$ ), a key effect commonly induced by adapter merging (e.g., the linear combination in Eq. 2).

**The TRAP<sup>2</sup> Objective** Let  $\Delta W$  denote the trainable LoRA update on top of a fixed base  $W_0$ . For a deployment

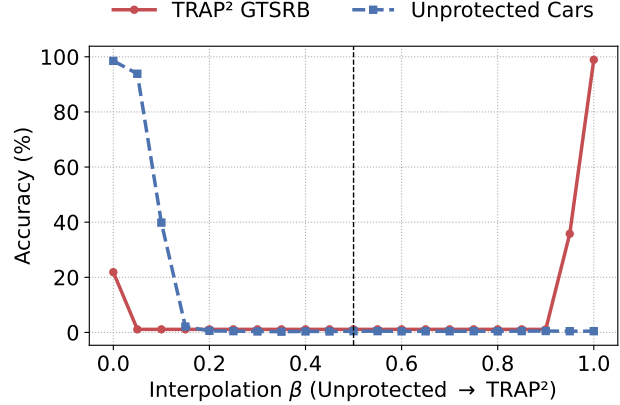


Figure 3. Performance degradation under pairwise merging. Accuracy along the interpolation path between an unprotected Cars adapter and a TRAP<sup>2</sup> GTSRB adapter is evaluated on both tasks.

scale  $s \in \mathbb{R}_{\geq 0}$ , let  $\mathcal{L}_{\text{scaled}}(\Delta W; s)$  denote the expected loss at scale  $s$ , as defined in Eq. (5). The nominal loss corresponds to the intended scale  $s = 1$ :

$$\mathcal{L}_{\text{nominal}}(\Delta W) := \mathcal{L}_{\text{scaled}}(\Delta W; 1).$$

Let  $\mathcal{S}$  be a distribution over off-nominal scales with support

$$\text{supp}(\mathcal{S}) \subseteq [s_{\min}, 1 - \delta] \cup [1 + \delta, s_{\max}],$$

where  $\delta \in \mathbb{R}_{>0}$  specifies an exclusion margin around the nominal scale  $s = 1$ . To control how strongly we penalize different off-nominal scales, we introduce a nonnegative weighting function  $w(s)$  and define the off-nominal loss as

$$\mathcal{L}_{\text{off}}(\Delta W) := \mathbb{E}_{s \sim \mathcal{S}} [w(s) \cdot \mathcal{L}_{\text{scaled}}(\Delta W; s)]. \quad (8)$$

Then, our goal is to minimize

$$J(\Delta W) = \mathcal{L}_{\text{nominal}}(\Delta W) - \lambda \cdot \mathcal{L}_{\text{off}}(\Delta W), \quad (9)$$

where  $\lambda \in \mathbb{R}_{>0}$  trades off standalone utility and sensitivity to re-scalings. The first term preserves intended deployment performance, while the second term induces sensitivity to off-nominal re-scalings, encouraging unmergeability.

**Unmergeability Mechanism** Eq. (9) intentionally creates an asymmetry across various scales: it preserves performance at  $s = 1$  by minimizing  $\mathcal{L}_{\text{nominal}}(\Delta W)$ , while increasing loss under off-nominal re-scalings via  $\mathcal{L}_{\text{off}}(\Delta W)$ . Because many merging operators effectively re-scale each constituent update (e.g., averaging scales each by  $1/N$ ), the merged adapter is pushed away from its nominal operating point; TRAP<sup>2</sup> is trained to be brittle under such shifts. The weighting function  $w(s)$  is used to normalize the training signal across scales. In particular, gradients can become small for down-scaled updates ( $s < 1$ ), so we set  $w(s) = 1/s$  by default to compensate for this effect and stabilize training.

Table 1. Standalone per-task accuracy (%) on 8 vision benchmarks for adapter-only deployment. We compare unprotected LoRA fine-tuning with post-hoc defenses (two LoRA variants of PaRaMS, Merge-Lock) and TRAP<sup>2</sup> across three CLIP backbones (ViT-B/32, ViT-L/14, ConvNeXt). For each dataset, bar length is normalized by the corresponding Fine-Tuned score (treated as 100), and bars below 95% of Fine-Tuned are colored pink. We omit the baselines for ConvNeXt since they are not directly applicable.

Backbone	Method	Cars	DTD	EuroSAT	GTSRB	MNIST	RESISC	Aircraft	SVHN	Average
ViT-B/32	Zero-Shot	59.397	44.096	45.481	32.255	47.988	60.302	18.962	31.384	42.483
	Fine-Tuned	99.523	68.723	98.259	98.416	99.087	93.048	51.725	96.168	87.994
	+ Merge-Lock*	0.575	2.394	10.963	2.009	9.462	3.540	11.423	9.666	6.254
	+ Merge-Lock <sup>†</sup>	0.482	2.074	6.333	2.059	9.988	2.111	1.140	9.066	4.157
	+ PaRaMS*	97.839	67.713	98.296	98.238	99.125	92.476	51.305	96.111	87.638
	+ PaRaMS <sup>†</sup>	92.150	61.596	92.222	97.694	98.125	91.127	46.685	95.534	84.392
	TRAP <sup>2</sup> (Ours)	99.829	66.117	98.519	98.911	99.462	93.302	52.355	96.557	88.132
ViT-L/14	Zero-Shot	77.864	55.532	62.259	50.713	76.162	71.365	32.583	58.552	60.629
	Fine-Tuned	99.767	76.702	98.778	98.466	99.587	95.587	72.577	97.758	92.403
	+ Merge-Lock*	0.497	2.340	8.593	3.256	11.737	1.571	0.930	6.473	4.425
	+ Merge-Lock <sup>†</sup>	0.389	1.862	9.111	1.880	11.950	1.635	1.110	8.259	4.525
	+ PaRaMS*	99.518	76.170	98.593	98.357	99.550	94.698	69.967	43.815	85.084
	+ PaRaMS <sup>†</sup>	98.912	74.043	98.407	98.248	99.638	93.397	67.027	41.424	83.887
	TRAP <sup>2</sup> (Ours)	99.876	78.830	98.481	99.584	99.438	96.175	80.138	97.167	93.711
ConvNeXt	Zero-Shot	89.554	59.628	54.519	48.892	54.888	67.143	27.512	34.327	54.558
	Fine-Tuned	98.492	76.436	98.926	99.268	99.325	96.063	59.226	97.105	90.605
	TRAP <sup>2</sup> (Ours)	97.606	76.064	98.630	98.931	99.488	94.079	64.326	96.159	90.660

**Optimization** As summarized in Algorithm 1, we optimize the TRAP<sup>2</sup> objective in Eq. (9) using stochastic first-order methods such as SGD. The expectation over  $s \sim \mathcal{S}$  is approximated by a single-sample Monte Carlo draw per iteration, which provides an unbiased gradient estimator for  $J$ . In Appendix A.1, we provide a stationarity guarantee for this procedure under standard assumptions.

**Degradation from Down-Scaling** Uniformly averaging  $N$  adapters re-scales each constituent adapter by a factor of  $1/N$ , placing the merged adapter away from the nominal scale. Since TRAP<sup>2</sup> explicitly amplifies loss under such off-nominal re-scalings, the merged one is expected to incur systematic degradation, as illustrated by the TRAP<sup>2</sup>-trained GTSRB adapter in Figure 3. This effect is formalized in Appendix A.2, which characterizes the loss increase under down-scaling (e.g.,  $s = 1/N$  in the uniform averaging).

**Cross-Adapter Degradation** Merging a TRAP<sup>2</sup>-trained adapter with an independently trained adapter moves the latter away from its nominal scale, as illustrated by the unprotected Cars adapter in Figure 3. Consequently, even an unprotected adapter can degrade after merging. Under mild regularity conditions, this degradation increases with the distance between the two adapters in parameter space. A formal analysis is deferred to Appendix A.4.

**Extension to Full Fine-Tuning** The same objective extends to full fine-tuning by defining a step-dependent update  $\Delta W_t := W_t - W_0$ . At each step  $t$ , we evaluate the nomi-

nal loss at  $W_t$  and an off-nominal loss at the scaled model  $W_0 + s \cdot \Delta W_t$ , and then update  $W_t$ . This yields a unified, architecture-agnostic formulation that applies to both adapter-based and full-checkpoint releases.

## 6. Experiments

In this section, we evaluate unmergeability under a realistic hub-style LoRA deployment setting, where a fixed base model is shared and only low-rank adapters are released and composed. Detailed settings (e.g., hyper-parameters) for experiments can be found in Appendix D.

### 6.1. Baselines

We compare TRAP<sup>2</sup> against two post-hoc defenses, PaRaMS (Junhao et al., 2025) and Merge-Lock (Wang et al., 2025). Since they are not LoRA-native, we use two adapter-only variants: (i) an *adapter-space* variant (\*) that transforms the released update  $\Delta W$  (for PaRaMS, this matches its LoRA setting using attention-head scaling only); and (ii) a *refitting* variant (†) that transforms  $W = W_0 + \Delta W$  and refits a rank- $r$  LoRA update via truncated SVD, which may incur approximation error. Detailed explanation for these baselines are provided in Appendix D.5.

### 6.2. Experiments on LoRA Merging

We consider eight standard vision classification benchmarks: Cars (Krause et al., 2013), DTD (Cimpoi et al., 2014), Eu-

Table 2. Averaged per-task accuracy (%) under 8-way LoRA merging: in each trial, the target-task adapter is protected and merged with seven unprotected adapters using TA/TIES/TIES+DARE/TSV/CART in Full/KNOTS/CORE spaces. Bars are normalized within each column, and values below 95% of *Unprotected* are highlighted in pink. We tune the merging coefficient via validation-based search over  $s \in \{0.1, 0.2, \dots, 10.0\}$  (including  $s=1.0$ ), making results optimistic for the merger.

Protection	Merging Method / Merging Space													
	TA		TIES			TIES+DARE			TSV			CART		
	Full	Full	KnOTS	Core	Full	KnOTS	Core	Full	KnOTS	Core	Full	KnOTS	Core	
<b>Backbone:</b> ViT-B/32 (Zero-shot: 42.483)														
<i>Unprotected</i>	48.273	48.020	49.925	53.264	48.180	49.926	54.745	51.442	49.202	55.014	49.553	49.850	51.201	
PaRaMS*	48.290	48.027	49.847	53.054	48.329	49.801	54.506	51.901	49.249	55.049	49.663	49.908	51.922	
PaRaMS <sup>†</sup>	48.104	48.078	49.872	53.022	48.208	49.872	54.080	51.418	49.033	54.509	49.418	49.791	50.647	
TRAP <sup>2</sup> (Ours)	23.121	36.480	37.514	37.213	33.880	28.383	36.752	24.815	24.210	24.449	41.324	40.967	41.602	
<b>Backbone:</b> ViT-L/14 (Zero-shot: 60.629)														
<i>Unprotected</i>	62.914	67.909	68.879	68.825	67.970	69.870	68.779	72.411	66.725	74.565	64.399	65.014	66.185	
PaRaMS*	62.926	67.821	69.583	69.229	67.915	69.631	69.215	71.985	66.740	74.592	64.358	65.012	66.231	
PaRaMS <sup>†</sup>	62.826	67.875	69.581	69.287	67.877	69.596	69.302	72.150	66.355	74.097	64.262	64.811	65.825	
TRAP <sup>2</sup> (Ours)	33.619	53.162	47.749	54.462	50.630	43.269	54.847	41.993	37.369	39.389	58.634	58.444	59.514	
<b>Backbone:</b> ConvNeXt (Zero-shot: 54.558)														
<i>Unprotected</i>	49.203	59.603	60.201	63.601	59.620	60.305	63.573	65.133	60.351	65.836	60.069	59.997	61.215	
TRAP <sup>2</sup> (Ours)	14.719	32.883	15.187	17.188	15.636	13.054	25.335	14.085	15.850	15.296	46.973	45.885	47.204	

roSAT (Helber et al., 2018), GTSRB (Stallkamp et al., 2012), MNIST (Deng, 2012), RESISC (Cheng et al., 2017), Aircraft (Maji et al., 2013), and SVHN (Netzer et al., 2011). We use CLIP (Radford et al., 2021) ViT-B/32 by default, and evaluate ViT-L/14 and ConvNeXt (Liu et al., 2022)-based CLIP models additionally. We fix the LoRA rank to  $r = 16$  and fine-tune only LoRA parameters on a frozen base model. For each task, we train (i) an unprotected adapter, to which post-hoc baselines are applied after fine-tuning, and (ii) a TRAP<sup>2</sup> adapter trained under Eq. (9).

After training, adapters are merged using TA (Ilharco et al., 2023), TIES (Yadav et al., 2023), TIES+DARE (Yu et al., 2024), TSV (Gargiulo et al., 2025), and CART (Choi et al., 2025), in Full space as well as KnOTS (Stoica et al., 2025) and Core Space (Panariello et al., 2025). Unless otherwise specified, we tune the merging coefficient via a simple grid search starting from 0.1 with step size 0.1 and select the best value on the validation set, using early stopping with patience 10. This procedure always evaluates the nominal coefficient 1.0 and spans both down-scaling and up-scaling of constituent updates, so the reported results reflect an optimistic (strong) merger that searches for the most favorable coefficient under each operator and space. Details of the merging operators and spaces are provided in Appendix B.

**Standalone Performance** A practical protection mechanism must preserve standalone utility under adapter-only deployment. Table 1 reports per-task standalone accuracy on the eight vision benchmarks for TRAP<sup>2</sup> and the two post-hoc baselines, PaRaMS and MergeLock, using the two variants described in Section 6.1.

MergeLock collapses under both variants, often yielding accuracy close to chance level even before merging, making it unsuitable for adapter-only deployment. In contrast, PaRaMS and TRAP<sup>2</sup> retain standalone performance comparable to unprotected fine-tuning across tasks, satisfying the standalone-utility requirement.

**Performance Degradation under Merging** Standalone utility alone does not guarantee unmergeability. Indiscriminate merging should yield a degraded merged model, potentially impairing both the protected task and other merged tasks. Table 2 reports controlled merging results averaged over eight trials, where we protect one target adapter, train the remaining seven unprotected, and then merge all eight adapters under each operator and space.

We quantify unmergeability by comparing each protected merging to the corresponding unprotected merging under the same operator and space. PaRaMS exhibits only small deviations from *Unprotected* across datasets and operators, indicating that task performance largely survives standard merging. In contrast, TRAP<sup>2</sup> incurs substantial post-merge degradation across settings, often pushing accuracy below the zero-shot baseline. Complete results are provided in Appendix C.

**Scaling and Architecture Generalization** We further evaluate robustness to backbone scale and architecture by repeating the same protocol on CLIP ViT-L/14 and ConvNeXt-based CLIP models. On ViT-L/14, TRAP<sup>2</sup> preserves strong standalone performance while still inducing sharp post-

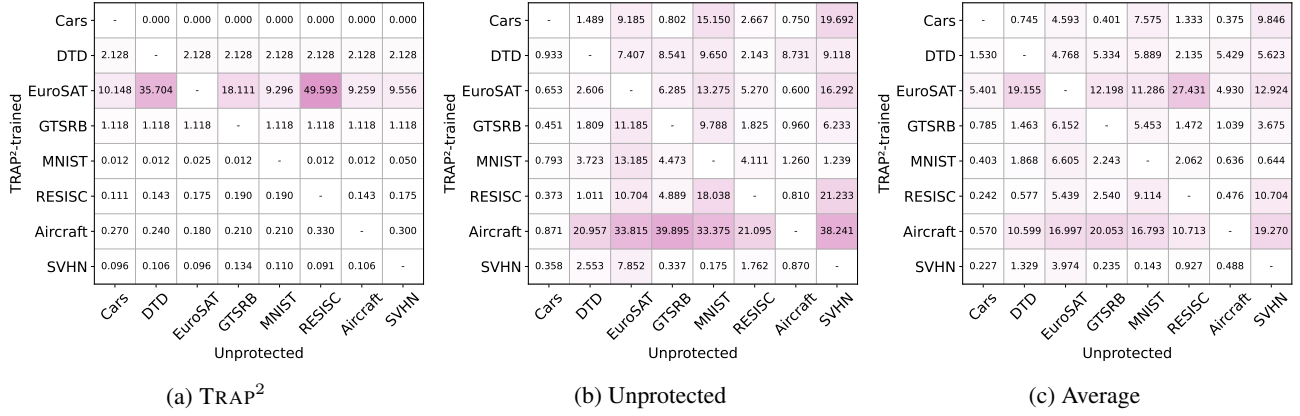


Figure 4. Results of pairwise LoRA merging at scale  $s = 0.8$  on CLIP ViT-B/32. Each cell merges one TRAP<sup>2</sup>-trained adapter for the row task with one unprotected adapter for the column task, and reports per-task accuracy (%; ↓) on (a) the protected task, (b) the unprotected task, and (c) their average. Cell color intensity encodes accuracy, with darker shading indicating lower accuracy (stronger degradation). The protected adapter consistently self-collapses after merging, often inducing collateral degradation on the unprotected task.

Table 3. Standalone per-task accuracy (%; ↑) on 8 vision benchmarks for CLIP ViT-B/32 under full fine-tuning. TRAP<sup>2</sup> preserves standalone performance comparable to standard fine-tuning.

Backbone	Method	Cars	DTD	EuroSAT	GTSRB	MNIST	RESISC	Aircraft	SVHN	Average
ViT-B/32	Zero-Shot	59.397	44.096	45.481	32.255	47.988	60.302	18.962	31.384	42.483
	Fine-Tuned	99.767	65.000	98.630	97.615	99.212	93.175	51.785	95.602	87.598
	TRAP <sup>2</sup> (Ours)	99.798	62.766	98.444	99.109	99.212	93.317	49.625	96.706	87.372

Table 4. Averaged per-task accuracy (%; ↓) on 8 vision benchmarks for CLIP ViT-B/32 under full-model merging. TRAP<sup>2</sup> remains effective under full fine-tuning, inducing strong degradation after merging compared to the unprotected baseline.

Protection	Merging Method				
	TA	TIES	TIES+DARE	TSV	CART
Backbone: ViT-B/32	(Zero-shot: 42.483)				
Unprotected	49.963	50.951	51.673	62.419	61.031
TRAP <sup>2</sup> (Ours)	28.475	37.970	37.899	38.181	42.116

merge degradation, whereas post-hoc baselines become unreliable under adapter-only deployment. On ConvNeXt, attention-symmetry-based defenses are not applicable, but TRAP<sup>2</sup> transfers without architectural assumptions and exhibits the same qualitative behavior, suggesting that the unmergeability effect persists across scale and architecture.

**Pairwise Merging** Following prior works (Junhao et al., 2025; Wang et al., 2025), we merge one TRAP<sup>2</sup>-trained adapter with one unprotected adapter and report per-task and average accuracy, as shown in Figure 4. Across task pairs, TRAP<sup>2</sup> consistently self-collapses: the protected-task accuracy drops sharply after merging, driving the decrease in average performance. We also observe collateral damage on the unprotected task, consistent with Theorems A.2 and A.4. Overall, TRAP<sup>2</sup> induces degradation even at the

two-adapter level, not only under large- $N$  composition.

### 6.3. Experiments on Full Model Merging

We further test whether TRAP<sup>2</sup> extends beyond LoRA by applying the same scaling objective during full fine-tuning on CLIP ViT-B/32 and then merging the resulting checkpoints via standard weight averaging. Table 3 reports standalone performance under full fine-tuning, showing that TRAP<sup>2</sup> preserves utility comparable to the unprotected baseline. Table 4 then evaluates full-model merging, where the merged model degrades reliably, mirroring the LoRA setting and indicating that the effect is not LoRA-specific.

### 6.4. Additional Analysis

We provide additional analysis to clarify which aspects of TRAP<sup>2</sup> are most responsible for its effectiveness and to assess robustness under stronger merging protocols.

**Uniform Averaging Proxy** We further test TRAP<sup>2</sup> with a uniform-averaging proxy, using update re-scaling as a lightweight pre-release check for merging behavior: uniform averaging of  $N$  adapters effectively scales each LoRA by  $s = 1/N$ . Figure 5 reports the resulting accuracy across eight vision datasets in ViT-B/32, where each subplot directly compares TRAP<sup>2</sup> against the vanilla baseline within the same dataset. Across all datasets, TRAP<sup>2</sup> exhibits a consistent catastrophic degradation once  $N \geq 2$ , while the

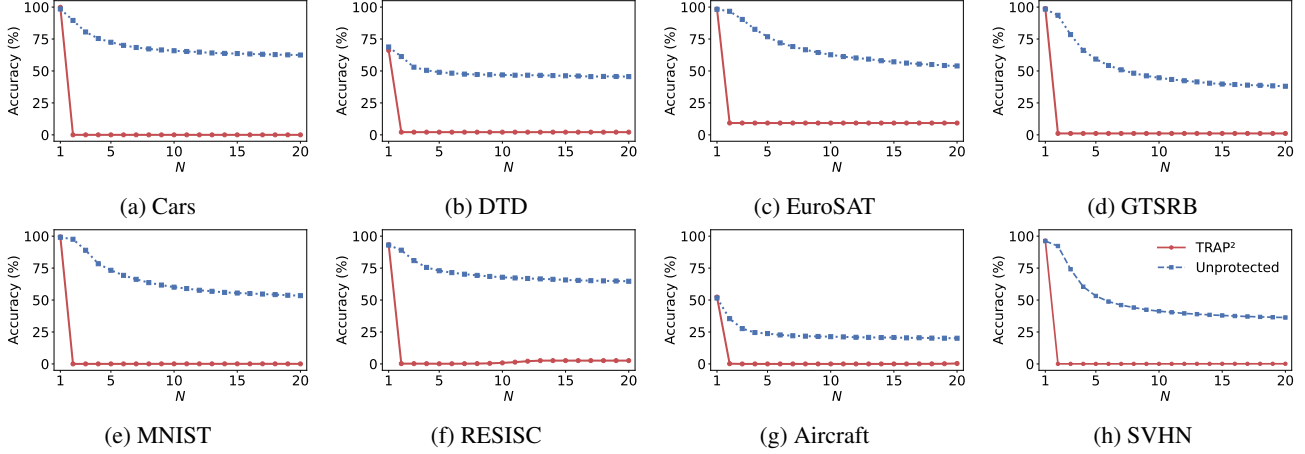


Figure 5. Uniform averaging proxy across 8 vision benchmarks. We simulate naive averaging of  $N$  adapters by scaling each adapter as  $s = 1/N$  before aggregation, and report accuracy (%) as a function of  $N$  for each dataset. TRAP<sup>2</sup> exhibits catastrophic degradation as soon as  $N \geq 2$ , while unprotected adapters remain relatively stable, indicating robustness of the protection against uniform averaging.

Table 5. Averaged accuracy (%; ↓) for data-dependent merging on CLIP ViT-B/32 (Full space). We evaluate RegMean and CoM using proxy datasets of 100 samples per task (R: random, C: class-stratified). TRAP<sup>2</sup> remains effective under data-dependent re-weighting, substantially degrading merged performance relative to the unprotected baseline.

Protection	Merging Method			
	RegMean (R)	RegMean (C)	CoM (R)	CoM (C)
Unprotected	49.107	49.036	64.776	66.599
TRAP <sup>2</sup> (Ours)	<b>9.480</b>	<b>9.386</b>	<b>32.331</b>	<b>32.918</b>

baseline remains largely stable as  $N$  increases. These results indicate that TRAP<sup>2</sup> remains effective against indiscriminate uniform averaging, a common plug-and-play reuse pattern in open adapter ecosystems.

**Data-dependent Merging Operators** Beyond standard merging operators, we evaluate TRAP<sup>2</sup> with two representative data-dependent mergers, RegMean (Jin et al., 2023) and Chain-of-Merges (CoM) (Buzzega et al., 2025). As shown in Table 5, TRAP<sup>2</sup> induces substantial post-merge degradation under both RegMean and CoM, suggesting that protection remains effective even when the merger leverages additional data signals. We also report the coefficients selected by CoM in Figure 6 as a diagnostic: unlike RegMean, CoM selects task-wise weights, and the coefficients show that it often assigns comparable or even larger weight to the TRAP<sup>2</sup>-protected adapter than to its unprotected counterpart, rather than down-weighting it to recover utility.

## 7. Conclusion

This paper studies protection of released fine-tuning updates against unauthorized post-release merging in model-

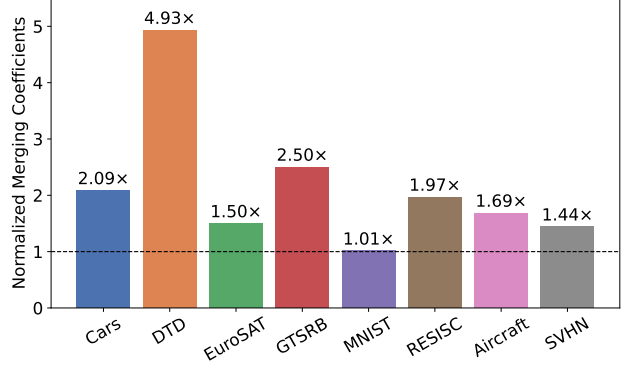


Figure 6. Normalized merging coefficients selected by CoM, when protecting each dataset-wise adapter with TRAP<sup>2</sup>. Each coefficient is normalized by the corresponding unprotected baseline, showing that data-driven re-weighting of CoM does not prevent the collapse of TRAP<sup>2</sup>-protected adapters under merging.

sharing ecosystems. We propose TRAP<sup>2</sup>, a training-time objective that embeds unmergeability directly into the released update by promoting sensitivity to off-nominal scaling, a lightweight proxy for the off-nominal coefficients and update transformations applied by common composition pipelines. Across experiments spanning architectures and release formats, TRAP<sup>2</sup> preserves strong standalone utility while consistently degrading performance under widely used merging operators, without requiring architecture-specific symmetries or access to full weights.

**Limitations** We evaluate protection primarily against hub-style, coefficient-based merging used for plug-and-play reuse. Extending TRAP<sup>2</sup> to remain effective under data-driven recovery, where a merger performs post-training with additional task-relevant data to restore utility, is an important direction for future work.

**Impact Statement** This paper proposes a training-time protection mechanism to discourage unauthorized or indiscriminate merging and to improve the integrity of adapter reuse in open ecosystems. Although our method uses adversarial perturbations during training, these are intended as a defensive tool for uploader protection, rather than to enable attacks. We do not anticipate negative societal impacts beyond those commonly associated with research on model security and responsible model sharing. However, as any protection mechanism may be misused (e.g., to disrupt third-party merging pipelines), we encourage responsible release practices such as clear labeling and usage guidelines. For example, a protected release can be accompanied by a short README stating that it is intended for standalone use and may not behave reliably under downstream merging.

## References

Bai, J., Chen, D., Qian, B., Yao, L., and Li, Y. Federated fine-tuning of large language models under heterogeneous tasks and client resources. In *The Thirty-eighth Annual Conference on Neural Information Processing Systems*, 2024. URL <https://openreview.net/forum?id=gkOzoHBXUw>.

Buzzega, P., Salami, R., Porrello, A., and Calderara, S. Rethinking layer-wise model merging through chain of merges, 2025. URL <https://arxiv.org/abs/2508.21421>.

Chen, S., Guo, Y., Ju, Y., Dalal, H., Zhu, Z., and Khisti, A. J. Robust federated finetuning of LLMs via alternating optimization of loRA. In *The Thirty-ninth Annual Conference on Neural Information Processing Systems*, 2025. URL <https://openreview.net/forum?id=e8DrPuJekZ>.

Cheng, G., Han, J., and Lu, X. Remote sensing image scene classification: Benchmark and state of the art. *Proceedings of the IEEE*, 105(10):1865–1883, 2017. doi: 10.1109/JPROC.2017.2675998.

Choi, J., Kim, D., Lee, C., and Hong, S. Revisiting weight averaging for model merging, 2025. URL <https://arxiv.org/abs/2412.12153>.

Cimpoi, M., Maji, S., Kokkinos, I., Mohamed, S., and Vedaldi, A. Describing textures in the wild. In *2014 IEEE Conference on Computer Vision and Pattern Recognition*, pp. 3606–3613, 2014. doi: 10.1109/CVPR.2014.461.

Cong, T., Ran, D., Liu, Z., He, X., Liu, J., Gong, Y., Li, Q., Wang, A., and Wang, X. Have you merged my model? on the robustness of large language model ip protection methods against model merging. In *Proceedings of the 1st ACM Workshop on Large AI Systems and Models with Privacy and Safety Analysis*, LAMPS ’24, pp. 69–76, New York, NY, USA, 2024. Association for Computing Machinery. ISBN 9798400712098. doi: 10.1145/3689217.3690614. URL <https://doi.org/10.1145/3689217.3690614>.

Deng, L. The mnist database of handwritten digit images for machine learning research [best of the web]. *IEEE Signal Processing Magazine*, 29(6):141–142, 2012. doi: 10.1109/MSP.2012.2211477.

Gargiulo, A. A., Crisostomi, D., Bucarelli, M. S., Scardapane, S., Silvestri, F., and Rodolà, E. Task singular vectors: Reducing task interference in model merging. In *2025 IEEE/CVF Conference on Computer Vision and Pattern Recognition (CVPR)*, pp. 18695–18705, 2025. doi: 10.1109/CVPR52734.2025.01742.

Hammoud, H. A. A. K., Michieli, U., Pizzati, F., Torr, P., Bibi, A., Ghanem, B., and Ozay, M. Model merging and safety alignment: One bad model spoils the bunch. In Al-Onaizan, Y., Bansal, M., and Chen, Y.-N. (eds.), *Findings of the Association for Computational Linguistics: EMNLP 2024*, pp. 13033–13046, Miami, Florida, USA, November 2024. Association for Computational Linguistics. doi: 10.18653/v1/2024.findings-emnlp.762. URL <https://aclanthology.org/2024.findings-emnlp.762>.

He, K., Zhang, X., Ren, S., and Sun, J. Deep residual learning for image recognition, 2015. URL <https://arxiv.org/abs/1512.03385>.

Helber, P., Bischke, B., Dengel, A., and Borth, D. Introducing eurosat: A novel dataset and deep learning benchmark for land use and land cover classification. In *IGARSS 2018 - 2018 IEEE International Geoscience and Remote Sensing Symposium*, pp. 204–207, 2018. doi: 10.1109/IGARSS.2018.8519248.

Hu, E. J., Shen, Y., Wallis, P., Allen-Zhu, Z., Li, Y., Wang, S., Wang, L., and Chen, W. LoRA: Low-rank adaptation of large language models. In *International Conference on Learning Representations*, 2022. URL <https://openreview.net/forum?id=nZeVKeeFYf9>.

Ilharco, G., Wortsman, M., Wightman, R., Gordon, C., Carlini, N., Taori, R., Dave, A., Shankar, V., Namkoong, H., Miller, J., Hajishirzi, H., Farhadi, A., and Schmidt, L. Openclip, July 2021. URL <https://doi.org/10.5281/zenodo.5143773>.

Ilharco, G., Ribeiro, M. T., Wortsman, M., Gururangan, S., Schmidt, L., Hajishirzi, H., and Farhadi, A. Editing models with task arithmetic, 2023. URL <https://arxiv.org/abs/2212.04089>.

Jin, X., Ren, X., Preotiu-Pietro, D., and Cheng, P. Data-less knowledge fusion by merging weights of language models. In *The Eleventh International Conference on Learning Representations*, 2023. URL <https://openreview.net/forum?id=FCnohuR6AnM>.

Junhao, W., Zhe, Y., and Jun, S. Disrupting model merging: A parameter-level defense without sacrificing accuracy, 2025. URL <https://arxiv.org/abs/2503.07661>.

Koo, J., Jang, M., and Ok, J. Towards robust and efficient federated low-rank adaptation with heterogeneous clients. In Che, W., Nabende, J., Shutova, E., and Pilehvar, M. T. (eds.), *Proceedings of the 63rd Annual Meeting of the Association for Computational Linguistics (Volume 1: Long Papers)*, pp. 416–429, Vienna, Austria, July 2025. Association for Computational Linguistics. ISBN 979-8-89176-251-0. doi: 10.18653/v1/2025.acl-long.19. URL <https://aclanthology.org/2025.acl-long.19/>.

Krause, J., Stark, M., Deng, J., and Fei-Fei, L. 3d object representations for fine-grained categorization. In *2013 IEEE International Conference on Computer Vision Workshops*, pp. 554–561, 2013. doi: 10.1109/ICCVW.2013.77.

Liu, Z., Mao, H., Wu, C.-Y., Feichtenhofer, C., Darrell, T., and Xie, S. A convnet for the 2020s. *Proceedings of the IEEE/CVF Conference on Computer Vision and Pattern Recognition (CVPR)*, 2022.

Loshchilov, I. and Hutter, F. Decoupled weight decay regularization. In *International Conference on Learning Representations*, 2019. URL <https://openreview.net/forum?id=Bkg6RiCqY7>.

maintainers, T. and contributors. Torchvision: Pytorch’s computer vision library. <https://github.com/pytorch/vision>, 2016.

Maji, S., Kannala, J., Rahtu, E., Blaschko, M., and Vedaldi, A. Fine-grained visual classification of aircraft. Technical report, 2013.

Mangrulkar, S., Gugger, S., Debut, L., Belkada, Y., Paul, S., Bossan, B., and Tietz, M. PEFT: State-of-the-art parameter-efficient fine-tuning methods. <https://github.com/huggingface/peft>, 2022.

Netzer, Y., Wang, T., Coates, A., Bissacco, A., Wu, B., and Ng, A. Y. Reading digits in natural images with unsupervised feature learning. In *NIPS Workshop on Deep Learning and Unsupervised Feature Learning 2011*, 2011. URL [http://ufldl.stanford.edu/housenumbers/nips2011\\_housenumbers.pdf](http://ufldl.stanford.edu/housenumbers/nips2011_housenumbers.pdf).

Panariello, A., Marczak, D., Magistri, S., Porrello, A., Twardowski, B., Bagdanov, A. D., Calderara, S., and van de Weijer, J. Accurate and efficient low-rank model merging in core space. In *Advances in Neural Information Processing Systems (NeurIPS)*, 2025.

Radford, A., Kim, J. W., Hallacy, C., Ramesh, A., Goh, G., Agarwal, S., Sastry, G., Askell, A., Mishkin, P., Clark, J., Krueger, G., and Sutskever, I. Learning transferable visual models from natural language supervision. In Meila, M. and Zhang, T. (eds.), *Proceedings of the 38th International Conference on Machine Learning*, volume 139 of *Proceedings of Machine Learning Research*, pp. 8748–8763. PMLR, 18–24 Jul 2021. URL <https://proceedings.mlr.press/v139/radford21a.html>.

Rosati, D., Wehner, J., Williams, K., Bartoszcze, L., Sajjad, H., and Rudzicz, F. Immunization against harmful fine-tuning attacks. In Al-Onaizan, Y., Bansal, M., and Chen, Y.-N. (eds.), *Findings of the Association for Computational Linguistics: EMNLP 2024*, pp. 5234–5247, Miami, Florida, USA, November 2024. Association for Computational Linguistics. doi: 10.18653/v1/2024.findings-emnlp.301. URL [https://aclanthology.org/2024.findings-emnlp.301/](https://aclanthology.org/2024.findings-emnlp.301).

Schuhmann, C., Beaumont, R., Vencu, R., Gordon, C. W., Wightman, R., Cherti, M., Coombes, T., Katta, A., Mullis, C., Wortsman, M., Schramowski, P., Kundurthy, S. R., Crowson, K., Schmidt, L., Kaczmarczyk, R., and Jitsev, J. LAION-5b: An open large-scale dataset for training next generation image-text models. In *Thirty-sixth Conference on Neural Information Processing Systems Datasets and Benchmarks Track*, 2022. URL <https://openreview.net/forum?id=M3Y74vmsMcY>.

Stallkamp, J., Schlipsing, M., Salmen, J., and Igel, C. Man vs. computer: Benchmarking machine learning algorithms for traffic sign recognition. *Neural Networks*, 32:323–332, 2012. ISSN 0893-6080. doi: <https://doi.org/10.1016/j.neunet.2012.02.016>. URL <https://www.sciencedirect.com/science/article/pii/S0893608012000457>. Selected Papers from IJCNN 2011.

Stoica, G., Ramesh, P., Ecsedi, B., Choshen, L., and Hoffman, J. Model merging with svd to tie the knots. *ICLR*, 2025.

Sun, Y., Li, Z., Li, Y., and Ding, B. Improving loRA in privacy-preserving federated learning. In *The Twelfth International Conference on Learning Representations*, 2024. URL <https://openreview.net/forum?id=NLPzL6HWn1>.

Vaswani, A., Shazeer, N., Parmar, N., Uszkoreit, J., Jones, L., Gomez, A. N., Kaiser, L. u., and Polosukhin, I. Attention is all you need. In Guyon, I., Luxburg, U. V., Bengio, S., Wallach, H., Fergus, R., Vishwanathan, S., and Garnett, R. (eds.), *Advances in Neural Information Processing Systems*, volume 30. Curran Associates, Inc., 2017. URL [https://proceedings.neurips.cc/paper\\_files/paper/2017/file/3f5ee243547dee91fb053c1c4a845aa-Paper.pdf](https://proceedings.neurips.cc/paper_files/paper/2017/file/3f5ee243547dee91fb053c1c4a845aa-Paper.pdf).

Wang, Z., Yang, E., Yin, L., Liu, S., and Shen, L. Model unmerging: Making your models unmergeable for secure model sharing, 2025. URL <https://arxiv.org/abs/2509.01548>.

Wolf, T., Debut, L., Sanh, V., Chaumond, J., Delangue, C., Moi, A., Cistac, P., Rault, T., Louf, R., Funtowicz, M., Davison, J., Shleifer, S., von Platen, P., Ma, C., Jernite, Y., Plu, J., Xu, C., Scao, T. L., Gugger, S., Drame, M., Lhoest, Q., and Rush, A. M. Transformers: State-of-the-art natural language processing. In *Proceedings of the 2020 Conference on Empirical Methods in Natural Language Processing: System Demonstrations*, pp. 38–45, Online, October 2020. Association for Computational Linguistics. URL <https://www.aclweb.org/anthology/2020.emnlp-demos.6>.

Xu, Z., Han, M., and Xing, W. EverTracer: Hunting stolen large language models via stealthy and robust probabilistic fingerprint. In Christodoulopoulos, C., Chakraborty, T., Rose, C., and Peng, V. (eds.), *Proceedings of the 2025 Conference on Empirical Methods in Natural Language Processing*, pp. 7019–7042, Suzhou, China, November 2025. Association for Computational Linguistics. ISBN 979-8-89176-332-6. doi: 10.18653/v1/2025.emnlp-main.358. URL <https://aclanthology.org/2025.emnlp-main.358/>.

Yadav, P., Tam, D., Choshen, L., Raffel, C., and Bansal, M. TIES-merging: Resolving interference when merging models. In *Thirty-seventh Conference on Neural Information Processing Systems*, 2023. URL <https://openreview.net/forum?id=xtaX3Wycj1>.

Yang, E., Shen, L., Wang, Z., Guo, G., Chen, X., Wang, X., and Tao, D. Representation surgery for multi-task model merging. *Forty-first International Conference on Machine Learning*, 2024.

Yu, L., Yu, B., Yu, H., Huang, F., and Li, Y. Language models are super mario: Absorbing abilities from homologous models as a free lunch. In *International Conference on Machine Learning*. PMLR, 2024.

## A. Theoretical Analysis of TRAP<sup>2</sup>

**Theorem A.1** (Stationarity of TRAP<sup>2</sup> under SGD). *Let  $J(\Delta W)$  be the TRAP<sup>2</sup> objective defined in Eq. (9), with a nonnegative weight  $w(s)$ . Assume  $J$  is  $L$ -smooth and bounded below by  $J_{\inf} > -\infty$ . Assume the scale distribution  $\mathcal{S}$  is supported on two off-nominal intervals: for  $0 < s_{\min} < 1 - \delta < 1 + \delta < s_{\max}$ ,*

$$\text{supp}(\mathcal{S}) \subseteq [s_{\min}, 1 - \delta] \cup [1 + \delta, s_{\max}].$$

Consider SGD with step size  $\eta \in (0, 1/L]$ :

$$\Delta W_{t+1} = \Delta W_t - \eta G_t.$$

Let  $\{(z_t, s_t)\}_{t \geq 0}$  be i.i.d. and define the filtration  $\mathcal{F}_t := \sigma(\Delta W_0, (z_0, s_0), \dots, (z_{t-1}, s_{t-1}))$ . Assume the stochastic gradient satisfies, almost surely,

$$\mathbb{E}[G_t | \mathcal{F}_t] = \nabla J(\Delta W_t), \quad \mathbb{E}[\|G_t - \nabla J(\Delta W_t)\|_F^2 | \mathcal{F}_t] \leq \sigma_w^2.$$

Then for any  $T \geq 1$ ,

$$\min_{0 \leq t \leq T-1} \mathbb{E}\|\nabla J(\Delta W_t)\|_F^2 \leq \frac{2(\mathbb{E}[J(\Delta W_0)] - J_{\inf})}{\eta T} + L\eta\sigma_w^2.$$

In particular, with  $\eta = \Theta(1/\sqrt{T})$ , we obtain

$$\min_{0 \leq t \leq T-1} \mathbb{E}\|\nabla J(\Delta W_t)\|_F^2 = O(1/\sqrt{T}).$$

Here,  $\sigma_w^2$  may depend on  $w$  and  $\text{supp}(\mathcal{S})$  (e.g., for  $w(s) = 1/s$ , it depends on  $s_{\min} > 0$ ).

*Proof.* By  $L$ -smoothness of  $J$ , for any  $t$ ,

$$J(\Delta W_{t+1}) \leq J(\Delta W_t) + \langle \nabla J(\Delta W_t), \Delta W_{t+1} - \Delta W_t \rangle + \frac{L}{2} \|\Delta W_{t+1} - \Delta W_t\|_F^2.$$

Using  $\Delta W_{t+1} - \Delta W_t = -\eta G_t$  yields

$$J(\Delta W_{t+1}) \leq J(\Delta W_t) - \eta \langle \nabla J(\Delta W_t), G_t \rangle + \frac{L\eta^2}{2} \|G_t\|_F^2.$$

Taking conditional expectation given  $\mathcal{F}_t$  and using  $\mathbb{E}[G_t | \mathcal{F}_t] = \nabla J(\Delta W_t)$ , we have

$$\mathbb{E}[\langle \nabla J(\Delta W_t), G_t \rangle | \mathcal{F}_t] = \langle \nabla J(\Delta W_t), \mathbb{E}[G_t | \mathcal{F}_t] \rangle = \|\nabla J(\Delta W_t)\|_F^2.$$

Moreover, by the conditional bias–variance decomposition,

$$\begin{aligned} \mathbb{E}[\|G_t\|_F^2 | \mathcal{F}_t] &= \|\mathbb{E}[G_t | \mathcal{F}_t]\|_F^2 + \mathbb{E}[\|G_t - \mathbb{E}[G_t | \mathcal{F}_t]\|_F^2 | \mathcal{F}_t] \\ &= \|\nabla J(\Delta W_t)\|_F^2 + \mathbb{E}[\|G_t - \nabla J(\Delta W_t)\|_F^2 | \mathcal{F}_t] \\ &\leq \|\nabla J(\Delta W_t)\|_F^2 + \sigma_w^2. \end{aligned}$$

Substituting these bounds gives

$$\mathbb{E}[J(\Delta W_{t+1}) | \mathcal{F}_t] \leq J(\Delta W_t) - \eta \left(1 - \frac{L\eta}{2}\right) \|\nabla J(\Delta W_t)\|_F^2 + \frac{L\eta^2}{2} \sigma_w^2.$$

Since  $\eta \leq 1/L$ , we have  $1 - \frac{L\eta}{2} \geq \frac{1}{2}$ , so that

$$\mathbb{E}[J(\Delta W_{t+1}) | \mathcal{F}_t] \leq J(\Delta W_t) - \frac{\eta}{2} \|\nabla J(\Delta W_t)\|_F^2 + \frac{L\eta^2}{2} \sigma_w^2.$$

Taking total expectation and summing over  $t = 0, \dots, T-1$  yields

$$\frac{\eta}{2} \sum_{t=0}^{T-1} \mathbb{E}\|\nabla J(\Delta W_t)\|_F^2 \leq \mathbb{E}[J(\Delta W_0)] - \mathbb{E}[J(\Delta W_T)] + \frac{L\eta^2}{2} \sigma_w^2 T.$$

Using  $J(\Delta W_T) \geq J_{\inf}$  and dividing by  $\eta T$  gives

$$\frac{1}{T} \sum_{t=0}^{T-1} \mathbb{E} \|\nabla J(\Delta W_t)\|_F^2 \leq \frac{2(\mathbb{E}[J(\Delta W_0)] - J_{\inf})}{\eta T} + L\eta\sigma_w^2.$$

Finally,  $\min_{0 \leq t \leq T-1} a_t \leq \frac{1}{T} \sum_{t=0}^{T-1} a_t$  for  $a_t \geq 0$  implies the claim.  $\square$

**Theorem A.2** (Self-degradation under Down-scaling). *Let  $\Delta W$  be an adapter trained on a data distribution  $\mathcal{D}$ , and recall  $\mathcal{L}_{\text{scaled}}(\Delta W; s)$  from Eq. (5). Fix any  $s \in (0, 1]$ . Assume that  $\mathcal{L}_{\text{scaled}}(\Delta W; \cdot)$  is twice differentiable on  $[s, 1]$  and that there exist constants  $\mu \in \mathbb{R}_{\geq 0}$  and  $\varepsilon \in \mathbb{R}_{\geq 0}$  such that*

$$\frac{\partial^2}{\partial u^2} \mathcal{L}_{\text{scaled}}(\Delta W; u) \geq \mu \quad \text{for all } u \in [s, 1], \quad \text{and} \quad \left| \frac{\partial}{\partial u} \mathcal{L}_{\text{scaled}}(\Delta W; 1) \right| \leq \varepsilon.$$

Then,

$$\mathcal{L}_{\text{scaled}}(\Delta W; s) - \mathcal{L}_{\text{scaled}}(\Delta W; 1) \geq \frac{\mu}{2}(1-s)^2 - \varepsilon(1-s).$$

In particular, if  $\frac{\mu}{2}(1-s) > \varepsilon$ , then  $\mathcal{L}_{\text{scaled}}(\Delta W; s) > \mathcal{L}_{\text{scaled}}(\Delta W; 1)$ .

*Proof.* The case  $s = 1$  is trivial, since both sides reduce to zero. Hence, without loss of generality, we assume that  $s < 1$ . Let  $g(u) := \mathcal{L}_{\text{scaled}}(\Delta W; u)$ . By the fundamental theorem of calculus,

$$g(s) - g(1) = \int_1^s g'(r) dr.$$

For any  $r \in [s, 1]$ , again by the fundamental theorem of calculus,

$$g'(r) - g'(1) = \int_1^r g''(v) dv = - \int_r^1 g''(v) dv \leq -\mu(1-r) = \mu(r-1),$$

where we used  $g''(v) \geq \mu$  on  $[s, 1]$ . Hence  $g'(r) \leq g'(1) + \mu(r-1)$ . Since  $s < 1$ , the integral is over a reversed interval and the inequality direction flips, giving

$$\int_1^s g'(r) dr \geq \int_1^s (g'(1) + \mu(r-1)) dr.$$

Evaluating the right-hand side yields

$$g(s) - g(1) \geq g'(1)(s-1) + \frac{\mu}{2}(s-1)^2.$$

Finally, using  $|g'(1)| \leq \varepsilon$  and  $s-1 = -(1-s)$  gives

$$g(s) - g(1) \geq -\varepsilon(1-s) + \frac{\mu}{2}(1-s)^2,$$

as desired. The sufficient condition  $\frac{\mu}{2}(1-s) > \varepsilon$  makes the right-hand side strictly positive.  $\square$

**Corollary A.3** (Self-degradation under Uniform Averaging). *Under the assumptions of Theorem A.2, if  $s = \frac{1}{N}$  (which corresponds to uniform averaging  $N$  adapters in the proxy analysis) for an integer  $N \geq 2$ , then*

$$\mathcal{L}_{\text{scaled}}\left(\Delta W; \frac{1}{N}\right) - \mathcal{L}_{\text{scaled}}(\Delta W; 1) \geq \frac{\mu}{2} \left(1 - \frac{1}{N}\right)^2 - \varepsilon \left(1 - \frac{1}{N}\right).$$

In particular, if  $\frac{\mu}{2} \left(1 - \frac{1}{N}\right) > \varepsilon$ , then  $\mathcal{L}_{\text{scaled}}(\Delta W; \frac{1}{N}) > \mathcal{L}_{\text{scaled}}(\Delta W; 1)$ .

**Remark** Theorem A.2 is stated for a generic adapter  $\Delta W$ . In our setting, TRAP<sup>2</sup> is trained to preserve performance at the nominal scale ( $s = 1$ ) while intentionally increasing the loss at off-nominal scales. As a result, when sweeping the scaling factor  $s \in (0, 1]$ , TRAP<sup>2</sup> exhibits a sharply increasing  $\mathcal{L}_{\text{scaled}}(\Delta W; s) - \mathcal{L}_{\text{scaled}}(\Delta W; 1)$  as  $s$  decreases, indicating pronounced self-degradation under down-scaling. In contrast, fine-tuning without protection remains largely insensitive to changes in  $s$ , as it optimizes only the nominal deployment without explicitly controlling off-nominal behavior. In Appendix C, we visualize  $\Delta \mathcal{L}(s)$  directly for both TRAP<sup>2</sup> and unprotected adapters. The consistently positive gaps for  $s < 1$  empirically support the prediction of Theorem A.2, i.e., when using TRAP<sup>2</sup>, down-scaling increases the loss.

**Theorem A.4** (Cross-adapter Collateral Damage). *For task  $\kappa$ , define the (nominal-scale) population loss*

$$L_\kappa(\Delta W) := \mathbb{E}_{\xi \sim \mathcal{D}_\kappa} [\ell(W_0 + \Delta W; \xi)].$$

Fix two distinct adapters  $\Delta W_\kappa$  and  $\Delta W_\tau$  with  $\kappa \neq \tau$ , and let  $V := \Delta W_\tau - \Delta W_\kappa$ . Let the merged adapter be

$$\overline{\Delta W} := \frac{1}{2}(\Delta W_\kappa + \Delta W_\tau) = \Delta W_\kappa + \frac{1}{2}V.$$

Assume  $L_\kappa$  is twice differentiable along the line segment  $\{\Delta W_\kappa + \gamma V/2 : \gamma \in [0, 1]\}$ . Define the weighted directional curvature along the merge path by

$$\mu_\kappa(V) := \frac{2}{\|V\|_F^2} \int_0^1 (1-\gamma) \left\langle V, \nabla^2 L_\kappa \left( \Delta W_\kappa + \frac{\gamma}{2}V \right) [V] \right\rangle d\gamma \quad (\text{for } V \neq 0).$$

Then for any  $\varepsilon \geq 0$  satisfying  $\|\nabla L_\kappa(\Delta W_\kappa)\|_F \leq \varepsilon$ ,

$$L_\kappa(\overline{\Delta W}) - L_\kappa(\Delta W_\kappa) \geq \frac{\mu_\kappa(V)}{8} \|V\|_F^2 - \frac{\varepsilon}{2} \|V\|_F.$$

In particular, if  $\nabla L_\kappa(\Delta W_\kappa) = 0$ , then

$$L_\kappa(\overline{\Delta W}) - L_\kappa(\Delta W_\kappa) \geq \frac{\mu_\kappa(V)}{8} \|\Delta W_\tau - \Delta W_\kappa\|_F^2.$$

*Proof.* Define  $\phi(\gamma) := L_\kappa(\Delta W_\kappa + \gamma V/2)$  for  $\gamma \in [0, 1]$ . By the chain rule,

$$\phi'(0) = \left\langle \nabla L_\kappa(\Delta W_\kappa), \frac{V}{2} \right\rangle, \quad \phi''(\gamma) = \frac{1}{4} \left\langle V, \nabla^2 L_\kappa \left( \Delta W_\kappa + \frac{\gamma}{2}V \right) [V] \right\rangle.$$

Using the integral form of Taylor's theorem,

$$\phi(1) - \phi(0) = \phi'(0) + \int_0^1 (1-\gamma)\phi''(\gamma) d\gamma.$$

For the curvature term,

$$\int_0^1 (1-\gamma)\phi''(\gamma) d\gamma = \frac{1}{4} \int_0^1 (1-\gamma) \left\langle V, \nabla^2 L_\kappa \left( \Delta W_\kappa + \frac{\gamma}{2}V \right) [V] \right\rangle d\gamma = \frac{\mu_\kappa(V)}{8} \|V\|_F^2.$$

For the linear term, by Cauchy–Schwarz and  $\|\nabla L_\kappa(\Delta W_\kappa)\|_F \leq \varepsilon$ ,

$$\phi'(0) = \left\langle \nabla L_\kappa(\Delta W_\kappa), \frac{V}{2} \right\rangle \geq -\frac{1}{2} \|\nabla L_\kappa(\Delta W_\kappa)\|_F \|V\|_F \geq -\frac{\varepsilon}{2} \|V\|_F.$$

Combining yields

$$\phi(1) - \phi(0) \geq \frac{\mu_\kappa(V)}{8} \|V\|_F^2 - \frac{\varepsilon}{2} \|V\|_F.$$

Since  $\phi(1) = L_\kappa(\overline{\Delta W})$  and  $\phi(0) = L_\kappa(\Delta W_\kappa)$ , the result follows.  $\square$

**Remark (Connection to TRAP<sup>2</sup>)** Theorem A.4 is agnostic to how adapters are trained. TRAP<sup>2</sup> is designed to *increase* merge-induced degradation by shaping the loss landscape so that, for many pairs  $(\kappa, \tau)$ , the secant direction  $V = \Delta W_\tau - \Delta W_\kappa$  yields a larger separation  $\|V\|_F$  and/or a larger positive average directional curvature  $\mu_\kappa(V)$ . As a result, the lower bound in Theorem A.4 becomes larger, amplifying collateral damage under naive merging.

**Remark (Interpretation of  $\mu_\kappa(V)$ )** The quantity  $\mu_\kappa(V)$  is an *average directional curvature* of  $L_\kappa$  along the merge path from  $\Delta W_\kappa$  to  $\overline{\Delta W}$  in the secant direction  $V$ . Unlike pointwise curvature lower bounds (e.g.,  $\langle V, \nabla^2 L_\kappa(\cdot)[V] \rangle \geq \mu \|V\|_F^2$  for all points),  $\mu_\kappa(V)$  summarizes curvature *only through a weighted average* required by the integral Taylor remainder.

**Remark (When does degradation become guaranteed?)** If  $\mu_\kappa(V) > 0$  and  $\|V\|_F > 4\varepsilon/\mu_\kappa(V)$ , then the right-hand side is positive, implying  $L_\kappa(\overline{\Delta W}) > L_\kappa(\Delta W_\kappa)$ . Thus, merge-induced degradation is more pronounced when adapters are far apart in weight space (large  $\|V\|_F$ ) and the source adapter is close to stationarity (small  $\varepsilon$ ).

**Remark (Empirical counterpart).** In experiments,  $L_\kappa$  and  $\nabla L_\kappa(\Delta W_\kappa)$  can be replaced by their empirical (or held-out) estimates. Correspondingly,  $\mu_\kappa(V)$  can be approximated either (i) from the loss profile along the merge path or (ii) via Hessian–vector products without forming the full Hessian. In Appendix C, we instantiate the former by evaluating the loss along the interpolation path  $\Delta W_\kappa + \beta(\Delta W_\tau - \Delta W_\kappa)$  for  $\beta \in [0, 1]$  and highlighting the midpoint  $\beta = \frac{1}{2}$ , and we further relate this empirical midpoint degradation to the secant distance  $V_{\text{norm}} = \|\Delta W_\tau - \Delta W_\kappa\|_F$  via correlation analysis.

## B. Merging Spaces and Merging Methods

In this section, we provide additional details on the merging operators and merging spaces used in our experiments.

### B.1. Merging Spaces

We consider three merging spaces: Full, KnOTS (Stoica et al., 2025), and Core (Panariello et al., 2025). Unless stated otherwise, each adapter update is represented as  $\Delta W_i = B_i A_i$  (Eq. (1)), and a merging operator  $\mathcal{M}(\cdot)$  produces a merged update, i.e.,  $\overline{\Delta W} = \mathcal{M}(\{\Delta W_i\}_{i=1}^N)$  (Eq. (6)).

**Full Space** In Full space, we merge directly in the weight-update space by materializing the full update  $\Delta W = BA \in \mathbb{R}^{d_{\text{out}} \times d_{\text{in}}}$  and applying the merging operator  $\mathcal{M}(\cdot)$  to  $\Delta W$  itself. This is convenient for off-line LoRA merging because it avoids any re-decomposition step back into low-rank factors.

A subtlety is that naive factor-space aggregation is not equivalent in general:  $(B_1 + B_2)(A_1 + A_2) \neq B_1 A_1 + B_2 A_2$  due to cross terms. Accordingly, prior works in federated fine-tuning (Sun et al., 2024; Bai et al., 2024; Koo et al., 2025; Chen et al., 2025) propose additional mechanisms to make factor-space aggregation well-defined. In contrast, we operate on the materialized updates in Full space, consistent with the task-vector view adopted by KnOTS (Stoica et al., 2025).

**KnOTS Space** KnOTS defines a shared right subspace from the collection of task updates. Given reconstructed updates  $\{\Delta W_i\}_{i=1}^N$  with  $\Delta W_i \in \mathbb{R}^{d_{\text{out}} \times d_{\text{in}}}$ , it forms the concatenated matrix

$$P := [\Delta W_1, \Delta W_2, \dots, \Delta W_N] \in \mathbb{R}^{d_{\text{out}} \times (N \cdot d_{\text{in}})},$$

and computes a low-rank SVD to obtain  $P \approx U \Sigma V^\top$ . Writing  $V = [V_1; \dots; V_N]$  as task-wise blocks (with  $V_i \in \mathbb{R}^{d_{\text{in}} \times k}$  corresponding to the  $i$ -th column block  $\Delta W_i$  in  $P$ ), KnOTS performs merging in this induced subspace by applying the merging operator to  $\{V_i\}_{i=1}^N$ , and reconstructs the merged update via the shared factors  $(U, \Sigma)$ .

**Core Space** Core merges adapters in a shared *bi-subspace* constructed from the LoRA factors. Given  $\Delta W_i = B_i A_i$  with rank  $r$ , it stacks the factors to build reference bases:

$$B_{\text{stack}} := [B_1, \dots, B_N] \in \mathbb{R}^{d_{\text{out}} \times (N \cdot r)}, \quad A_{\text{stack}} := [A_1; \dots; A_N] \in \mathbb{R}^{(N \cdot r) \times d_{\text{in}}}.$$

Then, it computes low-rank SVDs to obtain reference bases  $U_B^{\text{ref}}$  (left) and  $V_A^{\text{ref}}$  (right). Each task update is mapped into a compact core matrix

$$M_i := (U_B^{\text{ref}} B_i) (A_i V_A^{\text{ref}})^\top \in \mathbb{R}^{(N \cdot r) \times (N \cdot r)},$$

merging is performed over  $\{M_i\}_{i=1}^N$  in this core space, and the merged update is reconstructed as

$$\Delta W_{\text{merged}} := U_B^{\text{ref}} \mathcal{M}(\{M_i\}_{i=1}^N) V_A^{\text{ref}}.$$

### B.2. Merging Methods

We evaluate unmergeability using eight merging operators: TA (Ilharco et al., 2023), TIES (Yadav et al., 2023), DARE (Yu et al., 2024), TSV (Gargiulo et al., 2025), CART (Choi et al., 2025), RegMean (Jin et al., 2023), and CoM (Buzzeaga et al., 2025). Each operator takes a set of task updates (or their representations in a merging space) and returns a merged one. For concreteness, we denote each method in terms of task vectors  $\{\Delta W_i\}_{i=1}^N$ ; when operating in KnOTS/Core space,  $\Delta W_i$  is the corresponding representation in that space, which is finally mapped back to a full update.

**Task Arithmetic (TA)** TA merges by scaled summation:

$$\Delta W_{\text{merged}} = s \cdot \sum_{i=1}^N \Delta W_i, \quad W_{\text{merge}} = W_0 + \Delta W_{\text{merged}},$$

where  $s$  is a mixing coefficient (e.g.,  $s = 1/N$  for uniform averaging).

**TIES** Let  $\tau$  be a trimming ratio and let  $\text{Trim}_\tau(\cdot)$  zero out the smallest-magnitude entries so that only a fraction  $(1 - \tau)$  remains. TIES first trims each task vector and then resolves sign conflicts element-wise before averaging:

$$\widetilde{\Delta W}_i = \text{Trim}_\tau(\Delta W_i), \quad \Delta W_{\text{merged}} = \text{Agg}_{\text{sign}}\left(\{\widetilde{\Delta W}_i\}_{i=1}^N\right),$$

where  $\text{Agg}_{\text{sign}}(\cdot)$  keeps the dominating sign per coordinate and averages the remaining nonzero entries.

**DARE** Let  $m_i \in \{0, 1\}^{d_{\text{out}} \times d_{\text{in}}}$  be an i.i.d. Bernoulli mask with keep probability  $p$ . DARE randomly drops parameters and rescales the survivors:

$$\widetilde{\Delta W}_i = \frac{1}{p} (m_i \odot \Delta W_i), \quad \Delta W_{\text{merged}} = \mathcal{M}\left(\{\widetilde{\Delta W}_i\}_{i=1}^N\right),$$

where  $\odot$  denotes the Hadamard product, and  $\mathcal{M}(\cdot)$  is typically instantiated as TIES or TA.

**CART** Let  $W_i$  denote the  $i$ -th fine-tuned model and  $\bar{W} = \frac{1}{N} \sum_{i=1}^N W_i$  be their average. CART centers each task vector around  $\bar{W}$  and merges the low-rank components:

$$\Delta W_i^{\text{ctr}} := W_i - \bar{W}, \quad \Delta W_i^{(k)} := \text{LR}_k(\Delta W_i^{\text{ctr}}), \quad \Delta W_{\text{merged}} = s \cdot \sum_{i=1}^N \Delta W_i^{(k)},$$

where  $\text{LR}_k(\cdot)$  denotes a rank- $k$  approximation (e.g., truncated SVD).

**TSV** TSV first obtains low-rank factors  $\Delta W_i \approx U_i V_i^\top$  for each task and then orthogonalizes the concatenated components before reconstruction:

$$\Delta W_i \approx U_i V_i^\top, \quad U = [U_1, \dots, U_N], \quad \hat{U} = \text{Ortho}(U), \quad \Delta W_{\text{merged}} = \hat{U} \hat{V}^\top,$$

where  $\text{Ortho}(\cdot)$  denotes an orthogonalization procedure (e.g., QR decomposition), and  $\hat{V}$  collects the corresponding coefficients after projecting onto the orthogonalized basis.

**RegMean** RegMean is a data-dependent, layer-wise regression merger. Let  $\{W_i^{(l)}\}_{i=1}^N$  denote the weights of layer  $l$  from  $N$  task-specific models (or  $W_0^{(l)} + \Delta W_i^{(l)}$  in our notation), and let  $X_i^{(l)}$  be the input activations to layer  $l$  collected from task  $i$ . RegMean finds a merged layer  $W_{\text{merge}}^{(l)}$  by minimizing

$$\min_W \sum_{i=1}^N \left\| W X_i^{(l)} - W_i^{(l)} X_i^{(l)} \right\|_F^2,$$

which admits the closed-form solution

$$W_{\text{merge}}^{(l)} = \left( \sum_{i=1}^N W_i^{(l)} G_i^{(l)} \right) \left( \sum_{i=1}^N G_i^{(l)} \right)^{-1}, \quad G_i^{(l)} := X_i^{(l)} X_i^{(l)\top}.$$

**Chain of Merges (CoM)** CoM modifies RegMean to account for inter-layer dependencies by recomputing activation statistics after each layer merge. It proceeds sequentially from  $l = 1$  to  $L$ . For  $l = 1$ , the merged layer is computed as in RegMean using raw inputs  $X_i^{(1)}$ . For  $l \geq 2$ , CoM replaces  $X_i^{(l)}$  with the *post-merge* activations  $\hat{X}_i^{(l)}$  produced by the partially merged model:

$$\hat{X}_i^{(l)} = \sigma^{(l-1)} \left( W_{\text{merge}}^{(l-1)} \hat{X}_i^{(l-1)} \right),$$

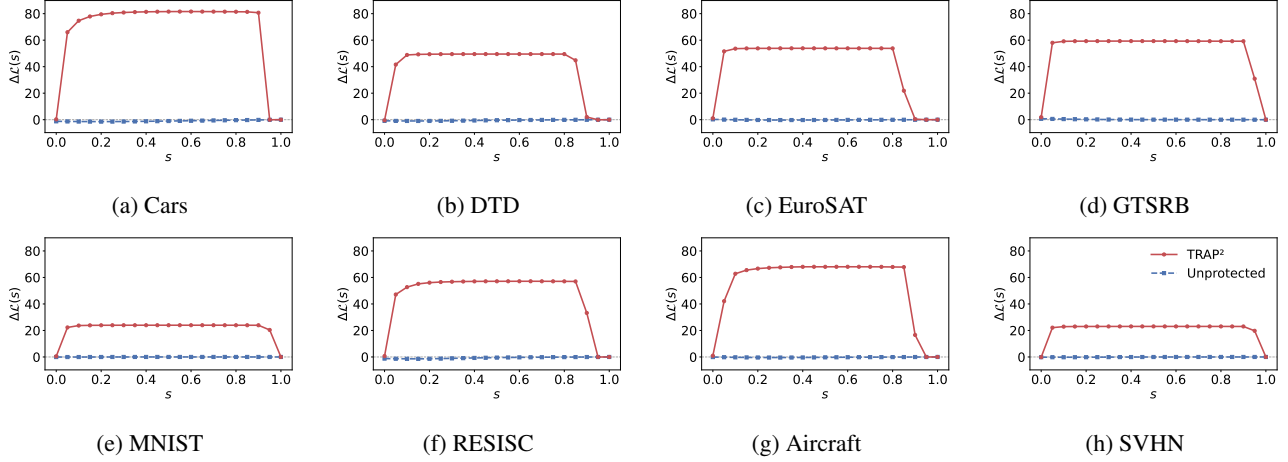


Figure 7. Scale-sweep of the loss change  $\Delta\mathcal{L}(s)$  relative to the nominal scale. Positive  $\Delta\mathcal{L}(s)$  for  $s < 1$  indicates self-degradation under down-scaling. Values near  $s = 1$  collapse to zero by design, as a small neighborhood around the nominal scale is excluded from  $\mathcal{S}$ .

and then computes the merged layer by the same regression rule with  $\hat{X}_i^{(l)}$ :

$$W_{\text{merge}}^{(l)} = \left( \sum_{i=1}^N W_i^{(l)} \hat{G}_i^{(l)} \right) \left( \sum_{i=1}^N \hat{G}_i^{(l)} \right)^{-1}, \quad \hat{G}_i^{(l)} := \hat{X}_i^{(l)} \hat{X}_i^{(l)\top}.$$

This autoregressive update mitigates the distribution shift caused by simultaneous merging with pre-merge activations.

## C. Additional Experiments

### C.1. Empirical Support for Theorems A.2 and A.4

In this subsection, we provide additional figures empirically supporting Theorems A.2 and A.4. We also connect these mechanisms to the failures in Figures 4 and 5. Figure 4 shows that even pairwise averaging can degrade performance, and Figure 5 shows the degradation worsens under uniform averaging as more adapters are merged.

To isolate the mechanism behind Figure 5, we report a scale-sweep plot (Figure 7) for a fixed adapter  $\Delta W$ . We sweep  $s \in [0, 1]$  and plot the loss change relative to the nominal scale,  $\Delta\mathcal{L}(s) := \mathcal{L}_{\text{scaled}}(\Delta W; s) - \mathcal{L}_{\text{scaled}}(\Delta W; 1)$ , so that  $\Delta\mathcal{L}(1) = 0$  by definition. Consistently positive  $\Delta\mathcal{L}(s)$  for  $s < 1$  indicates that down-scaling increases the loss, supporting Theorem A.2. Consequently, uniform averaging in Figure 4 can be harmful because it effectively down-scales each adapter.

Next, to mirror the pairwise setting in Figure 4, we report cross-adapter interpolation plots in Figure 8. Fixing two distinct adapters  $\Delta W_\kappa$  and  $\Delta W_\tau$ , we evaluate the loss along the line segment  $\Delta W_\kappa + \beta(\Delta W_\tau - \Delta W_\kappa)$  for  $\beta \in [0, 1]$ , and highlight the midpoint  $\beta = \frac{1}{2}$ , which corresponds to pairwise averaging. The increase in loss toward the midpoint is consistent with Theorem A.4 and provides a mechanistic explanation for the pairwise degradation observed in Figure 4.

To further connect Theorem A.4 to measurable quantities, we analyze the relationship between the secant distance between two adapters and the loss increase at the merge midpoint. For each pair  $(\kappa, \tau)$ , let  $V := \Delta W_\tau - \Delta W_\kappa$  and  $V_{\text{norm}} := \|V\|_F$ . We compute midpoint loss increases at  $\beta = \frac{1}{2}$  along the interpolation path  $\Delta W_\kappa + \beta(\Delta W_\tau - \Delta W_\kappa)$ , and summarize them as  $d\mathcal{L}_{\text{mid,mean}}$  and  $d\mathcal{L}_{\text{mid,max}}$ . Table 6 reports Spearman correlations and Pearson correlations (over  $\kappa \neq \tau$  pairs).

Together, the two figures and the table in this subsection decompose the empirical merging failures in Figures 4 and 5 into two interpretable effects: sensitivity to down-scaling (Theorem A.2) and sensitivity to cross-adapter mixing (Theorem A.4).

### C.2. Complete Results of Table 2, Table 5, and Figure 6

This subsection provides the complete results corresponding to the summarized results in Table 2 and Table 5. Specifically, Tables 7, 8, and 9 report the full results for the CLIP ViT-B/32, ViT-L/14, and ConvNeXt backbones, respectively (i.e., the complete version of Table 2). Tables 10 and 11 provide the full results corresponding to Tables 4 and 5, respectively.

## Making Models Unmergeable via Scaling-Sensitive Loss Landscape

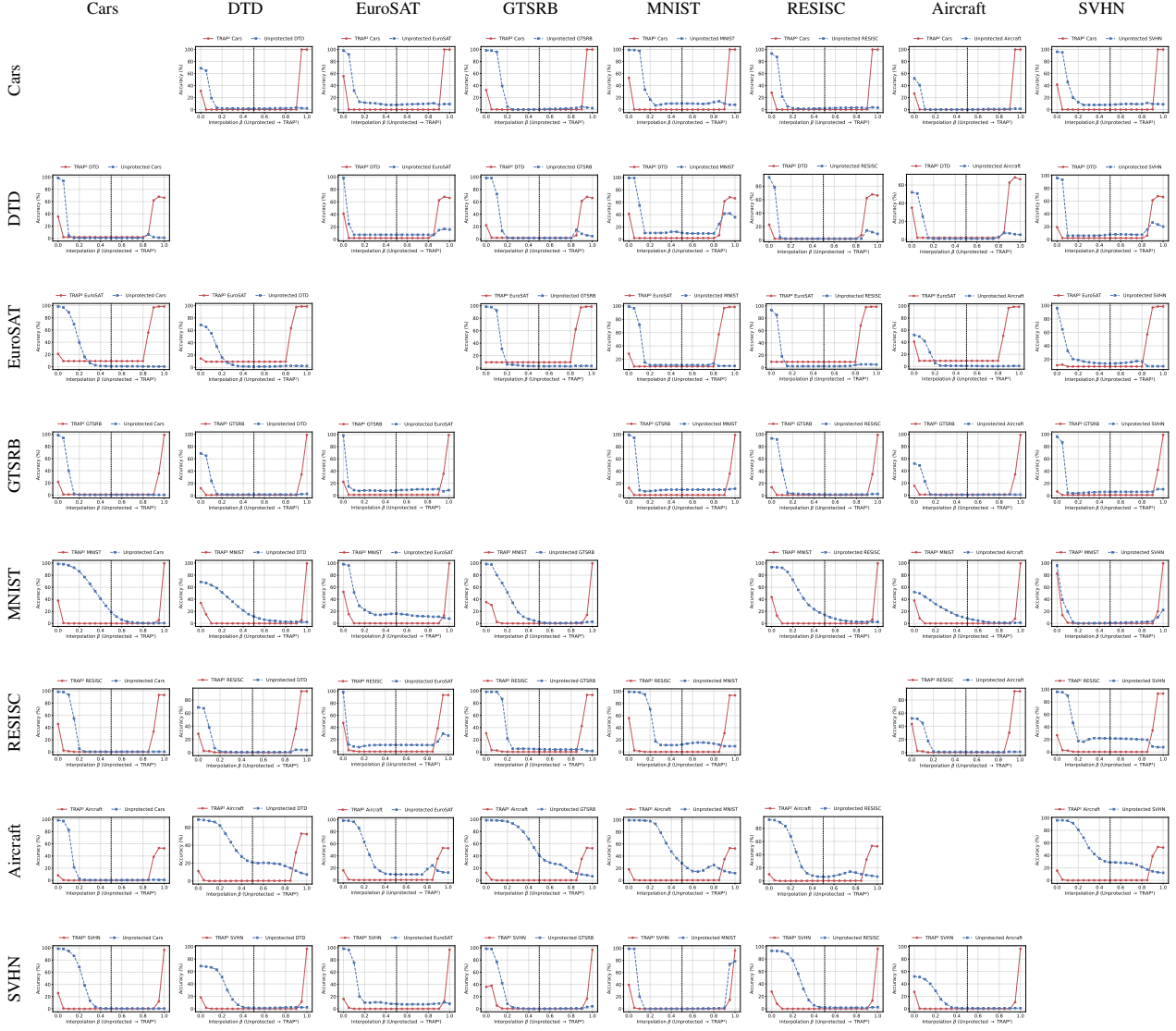


**Figure 8.** Pairwise interpolation matrix. Each off-diagonal cell sweeps the interpolation  $\Delta W_{\text{row}} + \beta(\Delta W_{\text{col}} - \Delta W_{\text{row}})$  with  $\beta \in [0, 1]$ , merging one TRAP<sup>2</sup>-trained adapter for the row task with one unprotected adapter for the column task. The midpoint  $\beta = 0.5$  corresponds to uniform averaging of the two adapters.

	$V_{\text{norm}}$	$d\mathcal{L}_{\text{mid,mean}}$	$d\mathcal{L}_{\text{mid,max}}$
<i>Spearman correlation</i> (nontrivial pairs, $n = 56$ )			
$V_{\text{norm}}$	1.000	0.741	0.682
$d\mathcal{L}_{\text{mid,mean}}$	0.741	1.000	0.958
$d\mathcal{L}_{\text{mid,max}}$	0.682	0.958	1.000
<i>Pearson correlation</i> (nontrivial pairs, $n = 56$ )			
$V_{\text{norm}}$	1.000	0.747	0.737
$d\mathcal{L}_{\text{mid,mean}}$	0.747	1.000	0.988
$d\mathcal{L}_{\text{mid,max}}$	0.737	0.988	1.000

**Table 6.** Correlation between the secant distance  $V_{\text{norm}} = \|\Delta W_{\tau} - \Delta W_{\kappa}\|_F$  and midpoint loss increase statistics. The positive correlation supports the intuition in Theorem A.4, i.e., larger separation in weight space tends to induce larger degradation at the merge midpoint.

Table 7. Averaged per-task accuracy (%; ↓) on 8 vision datasets using ViT-B/32. For each column (dataset), we apply the unmergeability protection technique *only* to the corresponding dataset, while all other datasets are trained with the standard (unprotected) procedure.

Merging	Space	Protection	Cars	DTD	EuroSAT	GTSRB	MNIST	RESISC	Aircraft	SVHN	Average
TA	Full	<i>Unprotected</i>					48.273				
		PaRaMS*	48.419	48.194	48.355	48.340	48.332	48.146	48.277	48.257	48.290
		PaRaMS <sup>†</sup>	47.922	48.326	47.987	48.177	47.904	48.207	48.133	48.175	48.104
		TRAP <sup>2</sup>	<b>13.355</b>	<b>16.803</b>	<b>17.854</b>	<b>16.706</b>	<b>28.491</b>	<b>25.044</b>	<b>39.451</b>	<b>27.264</b>	<b>23.121</b>
TIES	Full	<i>Unprotected</i>					48.020				
		PaRaMS*	48.078	47.945	48.138	48.142	48.121	47.912	47.911	47.969	48.027
		PaRaMS <sup>†</sup>	47.667	47.826	48.268	48.940	47.494	48.782	47.799	47.845	48.078
		TRAP <sup>2</sup>	<b>35.718</b>	<b>38.106</b>	<b>34.544</b>	<b>32.359</b>	<b>34.986</b>	<b>32.735</b>	<b>41.796</b>	<b>41.596</b>	<b>36.480</b>
TIES	KnOTS	<i>Unprotected</i>					49.925				
		PaRaMS*	49.645	49.936	49.908	50.169	49.877	49.932	49.589	49.718	49.847
		PaRaMS <sup>†</sup>	49.826	49.922	49.818	50.376	49.513	50.013	49.824	49.682	49.872
		TRAP <sup>2</sup>	<b>37.145</b>	<b>37.941</b>	<b>34.700</b>	<b>34.488</b>	<b>36.366</b>	<b>33.330</b>	<b>42.084</b>	<b>44.057</b>	<b>37.514</b>
TIES+DARE	Core	<i>Unprotected</i>					53.264				
		PaRaMS*	53.232	53.354	53.976	53.103	52.984	51.724	52.502	53.558	53.054
		PaRaMS <sup>†</sup>	51.681	52.109	53.934	55.847	53.533	51.219	51.810	54.044	53.022
		TRAP <sup>2</sup>	<b>35.866</b>	<b>38.002</b>	<b>35.895</b>	<b>32.493</b>	<b>36.048</b>	<b>32.729</b>	<b>42.435</b>	<b>44.238</b>	<b>37.213</b>
TIES+DARE	Full	<i>Unprotected</i>					48.180				
		PaRaMS*	48.585	48.140	48.153	48.368	48.665	48.364	47.874	48.483	48.329
		PaRaMS <sup>†</sup>	48.125	47.791	48.310	48.804	48.036	48.339	47.959	48.303	48.208
		TRAP <sup>2</sup>	<b>35.742</b>	<b>41.587</b>	<b>24.969</b>	<b>32.386</b>	<b>33.086</b>	<b>30.365</b>	<b>42.191</b>	<b>30.715</b>	<b>33.880</b>
TSV	KnOTS	<i>Unprotected</i>					49.926				
		PaRaMS*	49.613	49.913	49.880	50.115	49.896	49.947	49.557	49.485	49.801
		PaRaMS <sup>†</sup>	49.836	49.951	49.785	50.364	49.551	50.004	49.813	49.668	49.872
		TRAP <sup>2</sup>	<b>26.540</b>	<b>18.224</b>	<b>25.001</b>	<b>19.000</b>	<b>33.267</b>	<b>30.822</b>	<b>42.461</b>	<b>31.745</b>	<b>28.383</b>
TSV	Core	<i>Unprotected</i>					54.745				
		PaRaMS*	53.760	54.360	54.021	53.802	53.747	55.245	56.536	54.580	54.506
		PaRaMS <sup>†</sup>	52.428	52.144	55.416	55.822	54.253	53.991	53.903	54.682	54.080
		TRAP <sup>2</sup>	<b>37.636</b>	<b>46.398</b>	<b>31.414</b>	<b>26.365</b>	<b>36.050</b>	<b>32.623</b>	<b>42.744</b>	<b>40.784</b>	<b>36.752</b>
CART	Full	<i>Unprotected</i>					51.442				
		PaRaMS*	52.300	51.540	51.686	51.928	52.382	51.950	51.354	52.069	51.901
		PaRaMS <sup>†</sup>	50.749	51.429	51.455	52.052	51.615	50.866	51.017	52.162	51.418
		TRAP <sup>2</sup>	<b>21.166</b>	<b>7.817</b>	<b>19.764</b>	<b>14.604</b>	<b>32.600</b>	<b>28.426</b>	<b>43.745</b>	<b>30.397</b>	<b>24.815</b>
CART	KnOTS	<i>Unprotected</i>					49.202				
		PaRaMS*	49.264	49.185	49.233	49.236	49.306	49.286	49.145	49.334	49.249
		PaRaMS <sup>†</sup>	48.992	49.106	48.924	49.057	48.834	49.067	49.158	49.123	49.033
		TRAP <sup>2</sup>	<b>15.147</b>	<b>17.973</b>	<b>18.252</b>	<b>16.644</b>	<b>30.008</b>	<b>25.474</b>	<b>41.932</b>	<b>28.250</b>	<b>24.210</b>
CART	Core	<i>Unprotected</i>					55.014				
		PaRaMS*	55.082	54.769	55.170	55.124	55.090	55.103	54.929	55.124	55.049
		PaRaMS <sup>†</sup>	54.148	54.511	53.903	54.981	54.383	54.913	54.545	54.684	54.509
		TRAP <sup>2</sup>	<b>19.302</b>	<b>13.713</b>	<b>17.419</b>	<b>15.090</b>	<b>30.799</b>	<b>26.951</b>	<b>43.239</b>	<b>29.080</b>	<b>24.449</b>
CART	Full	<i>Unprotected</i>					49.553				
		PaRaMS*	49.704	49.555	49.652	49.749	49.726	49.549	49.735	49.633	49.663
		PaRaMS <sup>†</sup>	49.172	49.687	49.282	49.317	49.123	49.543	49.423	49.793	49.418
		TRAP <sup>2</sup>	<b>42.816</b>	<b>42.802</b>	<b>38.435</b>	<b>40.205</b>	<b>38.020</b>	<b>38.607</b>	<b>44.300</b>	<b>45.403</b>	<b>41.324</b>
CART	KnOTS	<i>Unprotected</i>					49.850				
		PaRaMS*	49.861	49.885	50.003	49.996	49.958	50.003	49.775	49.788	49.908
		PaRaMS <sup>†</sup>	49.710	49.765	49.753	49.796	49.591	49.944	49.714	50.054	49.791
		TRAP <sup>2</sup>	<b>41.984</b>	<b>42.729</b>	<b>38.214</b>	<b>39.815</b>	<b>37.888</b>	<b>38.131</b>	<b>44.075</b>	<b>44.896</b>	<b>40.967</b>
CART	Core	<i>Unprotected</i>					51.201				
		PaRaMS*	51.269	50.782	51.273	51.242	51.261	56.937	51.261	51.350	51.922
		PaRaMS <sup>†</sup>	50.538	50.684	50.561	50.429	50.442	50.590	50.638	51.292	50.647
		TRAP <sup>2</sup>	<b>42.963</b>	<b>43.063</b>	<b>38.670</b>	<b>40.324</b>	<b>38.099</b>	<b>38.855</b>	<b>45.173</b>	<b>45.672</b>	<b>41.602</b>

Table 8. Averaged per-task accuracy (%; ↓) on 8 vision datasets using ViT-L/14. For each column (dataset), we apply the unmergeability protection technique *only* to the corresponding dataset, while all other datasets are trained with the standard (unprotected) procedure.

Merging	Space	Protection	Cars	DTD	EuroSAT	GTSRB	MNIST	RESISC	Aircraft	SVHN	Average
TA	Full	<i>Unprotected</i>					62.914				
		PaRaMS*	62.879	62.902	62.809	63.009	62.895	63.026	62.846	63.039	62.926
		PaRaMS <sup>†</sup>	62.881	62.912	62.586	62.733	62.762	62.943	62.763	63.024	62.826
	Full	TRAP <sup>2</sup>	<b>27.473</b>	<b>5.044</b>	<b>37.021</b>	<b>41.930</b>	<b>37.699</b>	<b>42.751</b>	<b>41.111</b>	<b>35.924</b>	<b>33.619</b>
		<i>Unprotected</i>					67.909				
		PaRaMS*	67.997	67.837	67.562	67.762	67.672	67.822	67.773	68.140	67.821
TIES	KnOTS	PaRaMS <sup>†</sup>	67.886	68.315	67.755	67.656	67.629	67.629	67.964	68.168	67.875
		TRAP <sup>2</sup>	<b>52.952</b>	<b>56.880</b>	<b>53.079</b>	<b>56.687</b>	<b>51.841</b>	<b>47.531</b>	<b>57.770</b>	<b>48.556</b>	<b>53.162</b>
		<i>Unprotected</i>					68.879				
	Core	PaRaMS*	69.474	69.460	69.485	69.734	69.692	69.681	69.398	69.819	69.583
		PaRaMS <sup>†</sup>	69.906	70.001	69.261	69.671	69.204	69.747	69.201	69.657	69.581
		TRAP <sup>2</sup>	<b>53.246</b>	<b>5.854</b>	<b>54.261</b>	<b>56.986</b>	<b>52.333</b>	<b>48.442</b>	<b>58.650</b>	<b>52.222</b>	<b>47.749</b>
TIES+DARE	Full	<i>Unprotected</i>					68.825				
		PaRaMS*	70.013	69.207	69.981	69.541	68.468	68.208	68.839	69.575	69.229
		PaRaMS <sup>†</sup>	69.507	69.114	68.966	70.212	69.660	68.942	68.234	69.657	69.287
	KnOTS	TRAP <sup>2</sup>	<b>53.144</b>	<b>60.185</b>	<b>54.095</b>	<b>56.996</b>	<b>52.263</b>	<b>50.021</b>	<b>58.948</b>	<b>50.040</b>	<b>54.462</b>
		<i>Unprotected</i>					67.970				
		PaRaMS*	68.030	67.846	67.892	67.856	67.874	67.854	67.833	68.134	67.915
TSV	Core	PaRaMS <sup>†</sup>	67.862	68.310	67.734	67.545	67.643	67.740	68.063	68.116	67.877
		TRAP <sup>2</sup>	<b>52.942</b>	<b>56.854</b>	<b>53.068</b>	<b>49.655</b>	<b>45.670</b>	<b>46.878</b>	<b>57.735</b>	<b>42.238</b>	<b>50.630</b>
		<i>Unprotected</i>					69.870				
	KnOTS	PaRaMS*	69.476	69.538	69.571	69.747	69.782	69.738	69.386	69.811	69.631
		PaRaMS <sup>†</sup>	69.891	69.994	69.338	69.700	69.403	69.560	69.242	69.638	69.596
		TRAP <sup>2</sup>	<b>49.730</b>	<b>14.793</b>	<b>43.245</b>	<b>48.969</b>	<b>46.523</b>	<b>45.750</b>	<b>54.788</b>	<b>42.351</b>	<b>43.269</b>
CART	Full	<i>Unprotected</i>					68.779				
		PaRaMS*	70.032	69.163	70.002	69.548	68.345	68.218	68.856	69.556	69.215
		PaRaMS <sup>†</sup>	69.539	69.132	68.989	70.215	69.684	68.936	68.235	69.688	69.302
	Core	TRAP <sup>2</sup>	<b>53.108</b>	<b>60.187</b>	<b>53.506</b>	<b>55.934</b>	<b>52.482</b>	<b>56.741</b>	<b>58.777</b>	<b>48.038</b>	<b>54.847</b>
		<i>Unprotected</i>					72.411				
		PaRaMS*	71.921	72.166	71.541	72.490	72.392	72.040	71.147	72.186	71.985
TSV	KnOTS	PaRaMS <sup>†</sup>	71.595	71.627	71.154	71.095	74.594	72.036	71.991	73.110	72.150
		TRAP <sup>2</sup>	<b>49.354</b>	<b>9.318</b>	<b>41.842</b>	<b>46.996</b>	<b>46.687</b>	<b>47.285</b>	<b>53.230</b>	<b>41.233</b>	<b>41.993</b>
		<i>Unprotected</i>					66.725				
	Core	PaRaMS*	66.894	66.664	66.782	66.758	66.581	66.623	66.691	66.926	66.740
		PaRaMS <sup>†</sup>	66.446	66.327	66.201	65.923	66.376	66.238	66.488	66.840	66.355
		TRAP <sup>2</sup>	<b>37.811</b>	<b>5.794</b>	<b>38.412</b>	<b>42.787</b>	<b>44.325</b>	<b>45.750</b>	<b>46.253</b>	<b>37.819</b>	<b>37.369</b>
CART	Full	<i>Unprotected</i>					74.565				
		PaRaMS*	74.594	74.475	74.495	74.782	74.455	74.487	74.570	74.875	74.592
		PaRaMS <sup>†</sup>	74.234	74.000	73.956	73.853	74.139	73.869	74.171	74.556	74.097
	Core	TRAP <sup>2</sup>	<b>44.963</b>	<b>6.251</b>	<b>38.731</b>	<b>42.861</b>	<b>46.436</b>	<b>47.060</b>	<b>49.713</b>	<b>39.070</b>	<b>39.389</b>
		<i>Unprotected</i>					64.399				
		PaRaMS*	64.398	64.349	64.274	64.312	64.364	64.376	64.335	64.454	64.358
TSV	KnOTS	PaRaMS <sup>†</sup>	64.393	64.328	63.995	64.127	64.191	64.360	64.229	64.471	64.262
		TRAP <sup>2</sup>	<b>61.876</b>	<b>62.259</b>	<b>55.579</b>	<b>57.258</b>	<b>54.535</b>	<b>60.352</b>	<b>61.268</b>	<b>55.942</b>	<b>58.634</b>
		<i>Unprotected</i>					65.014				
	Core	PaRaMS*	64.864	65.028	64.938	65.052	64.978	65.094	65.000	65.145	65.012
		PaRaMS <sup>†</sup>	64.855	65.028	64.224	64.852	64.872	64.822	64.937	64.898	64.811
		TRAP <sup>2</sup>	<b>61.600</b>	<b>62.213</b>	<b>55.501</b>	<b>57.285</b>	<b>54.462</b>	<b>60.049</b>	<b>60.503</b>	<b>55.941</b>	<b>58.444</b>
CART	Full	<i>Unprotected</i>					66.185				
		PaRaMS*	66.192	66.223	66.186	66.278	66.357	66.204	66.144	66.264	66.231
		PaRaMS <sup>†</sup>	66.091	66.092	65.912	65.895	66.216	66.210	65.978	64.204	65.825
	Core	TRAP <sup>2</sup>	<b>62.274</b>	<b>62.748</b>	<b>55.842</b>	<b>57.657</b>	<b>54.726</b>	<b>60.537</b>	<b>61.656</b>	<b>60.671</b>	<b>59.514</b>

Table 9. Averaged per-task accuracy (%; ↓) on 8 vision datasets using ConvNeXt-CLIP. For each column (dataset), we apply the unmergeability protection technique *only* to the corresponding dataset, while all other datasets are trained with the standard (unprotected) procedure.

Merging	Space	Protection	Cars	DTD	EuroSAT	GTSRB	MNIST	RESISC	Aircraft	SVHN	Average
TA	Full	<i>Unprotected</i>					49.203				
		TRAP <sup>2</sup>	27.517	7.571	5.717	5.627	27.667	8.080	23.118	12.451	14.719
TIES	Full	<i>Unprotected</i>					59.603				
		TRAP <sup>2</sup>	38.137	22.408	24.832	31.501	43.896	26.516	38.894	36.884	32.883
TIES	KnOTS	<i>Unprotected</i>					60.201				
		TRAP <sup>2</sup>	35.288	4.705	6.059	6.200	45.138	7.610	7.350	9.149	15.187
TIES+DARE	Core	<i>Unprotected</i>					63.601				
		TRAP <sup>2</sup>	27.979	4.849	9.252	20.360	39.632	8.410	15.351	11.670	17.188
TIES+DARE	Full	<i>Unprotected</i>					59.620				
		TRAP <sup>2</sup>	23.064	6.336	5.693	7.802	42.015	7.855	14.633	17.690	15.636
TSV	KnOTS	<i>Unprotected</i>					60.305				
		TRAP <sup>2</sup>	25.330	5.845	6.021	5.719	35.552	7.601	9.201	9.162	13.054
TSV	Core	<i>Unprotected</i>					63.573				
		TRAP <sup>2</sup>	37.192	7.979	20.411	24.993	44.222	8.239	44.546	15.099	25.335
TSV	Full	<i>Unprotected</i>					65.133				
		TRAP <sup>2</sup>	22.530	5.425	4.833	8.953	31.513	6.969	20.963	11.495	14.085
CART	KnOTS	<i>Unprotected</i>					60.351				
		TRAP <sup>2</sup>	29.204	5.681	4.508	7.615	32.778	7.910	26.951	12.156	15.850
CART	Core	<i>Unprotected</i>					65.836				
		TRAP <sup>2</sup>	26.061	5.613	5.071	8.103	32.563	6.052	27.518	11.386	15.296
CART	Full	<i>Unprotected</i>					60.069				
		TRAP <sup>2</sup>	48.003	46.613	47.203	44.142	47.361	45.495	51.944	45.026	46.973
CART	KnOTS	<i>Unprotected</i>					59.997				
		TRAP <sup>2</sup>	45.126	46.136	45.751	42.764	46.963	44.119	51.613	44.611	45.885
CART	Core	<i>Unprotected</i>					61.215				
		TRAP <sup>2</sup>	48.183	47.016	47.374	44.171	47.527	46.041	52.126	45.192	47.204

Table 10. Averaged per-task accuracy (%; ↓) on 8 vision datasets using ViT-B/32 via full fine-tuning. For each column (dataset), we apply the unmergeability protection technique *only* to the corresponding dataset, while all other datasets are trained with the standard (unprotected) procedure.

Merging	Space	Protection	Cars	DTD	EuroSAT	GTSRB	MNIST	RESISC	Aircraft	SVHN	Average
TA	Full	<i>Unprotected</i>					49.963				
		TRAP <sup>2</sup>	26.951	14.830	26.757	19.022	35.705	30.731	41.739	32.064	28.475
TIES	Full	<i>Unprotected</i>					50.951				
		TRAP <sup>2</sup>	34.800	42.105	31.460	37.038	39.769	35.985	41.609	40.995	37.970
TIES+DARE	Full	<i>Unprotected</i>					51.673				
		TRAP <sup>2</sup>	34.780	42.093	37.448	37.068	39.756	32.395	41.934	37.715	37.899
TSV	Full	<i>Unprotected</i>					62.419				
		TRAP <sup>2</sup>	37.256	40.708	38.460	34.513	39.847	33.909	43.632	37.125	38.181
CART	Full	<i>Unprotected</i>					61.031				
		TRAP <sup>2</sup>	41.616	43.699	38.800	41.086	42.441	41.291	44.668	43.326	42.116

Table 11. Averaged per-task accuracy (%; ↓) on 8 vision datasets using ViT-B/32. For each column (dataset), we apply the unmergeability protection technique *only* to the corresponding dataset, while all other datasets are trained with the standard (unprotected) procedure. For each merging method, Gram matrices are computed using 100 validation samples per task. (R) indicates random sampling, and (C) denotes class-wise stratified sampling for constructing proxy datasets.

Merging	Space	Protection	Cars	DTD	EuroSAT	GTSRB	MNIST	RESISC	Aircraft	SVHN	Average
RegMean (R)	Full	<i>Unprotected</i> TRAP <sup>2</sup>	4.345	3.993	6.812	4.333	20.862	7.330	22.835	5.327	9.480
RegMean (C)	Full	<i>Unprotected</i> TRAP <sup>2</sup>	4.286	3.993	6.826	4.339	20.801	7.434	22.362	5.050	9.386
CoM (R)	Full	<i>Unprotected</i> TRAP <sup>2</sup>	43.587	38.420	42.622	7.976	20.866	36.429	49.375	19.372	32.331
CoM (C)	Full	<i>Unprotected</i> TRAP <sup>2</sup>	45.061	40.453	35.931	7.242	30.063	33.749	51.684	19.164	32.918

## D. Implementation Details

### D.1. Datasets

We conduct experiments on a collection of eight standard image classification benchmarks, including Cars (Krause et al., 2013), DTD (Cimpoi et al., 2014), EuroSAT (Helber et al., 2018), GTSRB (Stallkamp et al., 2012), MNIST (Deng, 2012), RESISC (Cheng et al., 2017), Aircraft (Maji et al., 2013), and SVHN (Netzer et al., 2011). These datasets span fine-grained recognition, textures, remote sensing, traffic signs, and handwritten digits, providing a comprehensive testbed for evaluating adapter merging under diverse visual domains. We follow the standard train/validation/test splits and evaluation protocols used in prior CLIP-based studies. Specifically, for Cars, GTSRB, MNIST, and SVHN, we use the official split provided by KnOTS (Stoica et al., 2025), where the validation set is formed by holding out 20% of the original test set. For DTD, we use the first split among the 10 pre-defined splits, following TA (Ilharco et al., 2023). For RESISC and Aircraft, we use the only available official split as-is. For EuroSAT, we adopt the split protocol from Representation Surgery (Yang et al., 2024). All dataloaders are implemented using TorchVision (maintainers & contributors, 2016) library.

### D.2. Architectures

We use pre-trained CLIP models (Radford et al., 2021) with three visual encoders: ViT-B/32, ViT-L/14, and ConvNeXt. Specifically, we use checkpoints from OpenAI for ViT-B/32<sup>1</sup> and ViT-L/14<sup>2</sup>, which are loaded via the HuggingFace Transformers (Wolf et al., 2020) library. For ConvNeXt (Liu et al., 2022), we utilize OpenCLIP (Ilharco et al., 2021) to load the checkpoint<sup>3</sup> trained with a subset of LAION-5B (Schuhmann et al., 2022).

### D.3. Fine-tuning with LoRA

Via HuggingFace PEFT (Mangrulkar et al., 2022) library, we insert LoRA adapters into the vision encoder and optimize *only* the LoRA parameters. All pre-trained CLIP weights are frozen, including the entire text encoder, following KnOTS (Stoica et al., 2025). For ViT-based visual backbones, we apply LoRA to the self-attention projections (Q, K, V, and O). For ConvNeXt backbones, we apply LoRA to the  $1 \times 1$  pointwise convolution layers. We optimize with AdamW (Loshchilov & Hutter, 2019), using an initial learning rate of  $3 \times 10^{-4}$  with a cosine schedule and warmup. We set  $\delta = 0.05$ ,  $s_{\min} = 0.05$ , and  $s_{\max} = 2.0$ . We use  $\lambda \in \{0.01, 0.001\}$ , selected per dataset via grid search on a validation split. We use rank  $r = 16$  with scaling factor  $\alpha = r$ , so the nominal (authorized) LoRA scale  $s = \alpha/r$  equals 1. We use no LoRA bias and set the LoRA dropout rate to 0.1.

### D.4. Full Fine-tuning

For full fine-tuning, we optimize with AdamW, using an initial learning rate of  $1 \times 10^{-4}$  with a cosine schedule and warmup. We update all parameters in the vision encoder. We use  $\lambda \in \{0.05, 0.01, 0.005, 0.001\}$ , selected per dataset via

<sup>1</sup><https://huggingface.co/openai/clip-vit-base-patch32>

<sup>2</sup><https://huggingface.co/openai/clip-vit-large-patch14>

<sup>3</sup>[https://huggingface.co/laion/CLIP-convnext\\_base\\_w-laion2B-s13B-b82K-augreg](https://huggingface.co/laion/CLIP-convnext_base_w-laion2B-s13B-b82K-augreg)

grid search on a validation split. We set  $\delta = 0.05$ ,  $s_{\min} = 0.05$ , and  $s_{\max} = 2.0$ .

## D.5. Post-hoc Baselines

We compare against two post-hoc protection baselines, PaRaMS (Junhao et al., 2025) and Merge-Lock (Wang et al., 2025). Following Section 4, for each method we evaluate two LoRA adaptations: (i) an adapter-space variant ( $^*$ ) that applies the post-hoc transform only to the released adapter update  $\Delta W$ , and (ii) a refitting variant ( $^{\dagger}$ ) that applies the original transform to the full updated weights  $W = W_0 + \Delta W$  and then refits a LoRA adapter via low-rank projection (truncated SVD), which may introduce approximation error.

**PaRaMS $^*$**  We apply PaRaMS to the LoRA adapter weights  $\Delta W$  after fine-tuning. In the LoRA setting of PaRaMS, PEM-based task arithmetic merges only LoRA-adapted parameters. Since this part can be viewed as the multiplication of two matrices, PaRaMS applies the scaling module only and does not use rearrangement in this setting (Junhao et al., 2025). Accordingly, our LoRA-native PaRaMS instantiation applies only per-head diagonal rescaling to  $\Delta W$  in the adapter space. We instantiate the uniform scaling range as  $[0.5, 1.5]$ .

**Merge-Lock $^*$**  Merge-Lock uses paired-cancellation transforms in self-attention with general linear mappings. Each transform matrix is constructed as  $T = RPD$ , where  $R$  is a random mixing matrix,  $P$  is a permutation matrix, and  $D$  is a diagonal scaling matrix (Wang et al., 2025). This construction increases parameter mismatch while preserving functional equivalence in the original full-weight setting (Wang et al., 2025). In our LoRA-native instantiation, we apply the same QK and VO mappings directly to  $\Delta W$ . In this setting, the original function-preservation guarantee may not strictly hold due to cross terms with the frozen base weights, as discussed in Section 4. For  $D$ , we use log-normal diagonal scaling with log-standard deviation 0.2 and clip scaling factors below  $10^{-4}$  for numerical stability to avoid near-singular matrices. In our implementation, we draw  $R$  with i.i.d. standard normal entries and sample  $P$  uniformly at random, without tuning additional hyperparameters for these components.

**PaRaMS $^{\dagger}$**  After fine-tuning, we apply the PaRaMS self-attention rescaling to the full updated weights  $W = W_0 + \Delta W$ , and then refit a LoRA adapter via truncated SVD. As above, we use uniform diagonal rescaling in  $[0.5, 1.5]$ .

**Merge-Lock $^{\dagger}$**  Analogously, we apply the Merge-Lock full-space transform to  $W = W_0 + \Delta W$  using the  $T = RPD$  construction, and then refit a LoRA adapter using truncated SVD. For  $D$ , we use the same log-normal diagonal scaling with log-standard deviation 0.2, and clip scaling factors below  $10^{-4}$  for numerical stability. We use the same sampling scheme for  $R$  and  $P$  as above.

## D.6. Merging

Unless otherwise specified, we sweep the merging coefficient from 0.1 to 10.0 in increments of 0.1 and select the best value on the validation set. To reduce compute, we stop the sweep early if the validation metric does not improve for 10 consecutive grid points (patience 10), while always evaluating the nominal coefficient 1.0. For the pair-wise merging experiments in Figure 4, we set the merging coefficient to 0.8 for both adapters, following PaRaMS (Junhao et al., 2025).

For dataset-dependent merging methods (e.g., RegMean and CoM) in Table 5 and Figure 6, we sample 100 datapoints per dataset to estimate the required statistics. We consider two sampling strategies: uniform random sampling (R) and class-wise stratified sampling (C). For datasets with more than 100 classes, we first select 100 classes and then sample one example per selected class.

For TIES, we sweep the pruning ratio from 100% down to 10% in steps of 10%. For TIES-DARE variants, we additionally sweep the pruning coefficient over  $\{10^{-5}, 0.1, 0.2, 0.3, 0.4, 0.5, 0.6, 0.7, 0.8, 0.9\}$ , where  $10^{-5}$  approximates the no-pruning regime. For CART, we sweep the pruning ratio over  $\{0.04, 0.08, 0.16, 0.32\}$ .